U.PORTO

FEUP FACULDADE DE ENGENHARIA
UNIVERSIDADE DO PORTO

INTEGRATED MASTER ENVIRONMENTAL ENGINEERING

2014/2015

Adsorption equilibrium and fixed-bed adsorption of phenolic acids onto polymeric adsorbent

Sílvia Vanessa dos Santos Barbosa

Dissertation for the Degree

Master in Environmental Engineering

Supervisor: **Professor Alírio Rodrigues**

Co-Supervisor: **Dr. Paula Pinto**

Developed at:

Laboratory of Separation and Reaction Engineering

LABORATÓRIO ASSOCIADO

LSRE LABORATORY OF SEPARATION AND REACTION ENGINEERING

Laboratory of Catalysis and Materials LCM

Acknowledgments

I would like start to thank my supervisors Professor Alírio Rodrigues and Dr. Paula Pinto for giving all necessary instructions and for having continuously monitored the progress of my work. I am very grateful for all the availability, patience and motivation, especially in times of increased anxiety and workload.

I would like to make a very special thanks to Inês Mota for being such a helpful co-worker. Despite all the setbacks and adversities that happened throughout this work, she never failed in giving me all the necessary help and cooperation. I am also very grateful for all the transmitted knowledge, friendliness, optimism and enthusiasm that allowed me to do this dissertation in a truly enviable working environment.

I also have to make a sincere thanks to all of my laboratory partners (Fatiha, Cátia, Elson and Carina), that dealt directly with me, for always being so helpful in any situation and for the fantastic mood that permitted an excellent working environment.

I want thanking to all my friends (Ana, Francisca, Marta, Inês, Nuno, Filipe, João Vaz e João Martins) for the good moments spent and for always having been a source of happiness and encouragement. Especially for Rita, to be present at all times and always be ready to listen to me and to give a friend advice.

At last, a special thanks to my boyfriend Carlos Sousa, my mother Lúcia Santos, and my best friend Cristiana Reis, for being there in all moments and who supported me all the way through and helped me believe I could finish the project.

I declare, under oath, that this work is original and that all non-original contributions were properly referenced with their source correctly identified.

Sílvia Vanessa Santos Barbosa

Porto, 29 de Junho de 2015

Abstract

Phenolic acids such as vanillic acid (VA) and syringic acid (SA) result from lignin oxidation with O_2 in alkaline medium, a process focused mainly for vanillin (VL) and syringaldehyde (SY) production. Studies of separation and recovery of VA and SA are scarce. However, these two phenolic acids have many applications on pharmaceutical industry and their possible recovery from lignin oxidation mixture needs to be investigated. The main purpose of this thesis was to study the adsorption of VA and SA in a non-polar resin, Sepabeads SP700, aiming their separation from the other products and recovery.

Batch equilibrium adsorption experiments were carried out at three different temperatures (288, 298 and 333 K) for aqueous solutions of VA and SA and experimental results were fitted by Langmuir and Freundlich adsorption equilibrium isotherms.

The maximum adsorption capacity obtained with the Langmuir model was 0.475 g/g to VA and 0.391 g/g to SA. With the Freundlich model, it was obtained a 1/n of 0.383 and 0.396 for VA and SA, respectively. This model predicted better the q_e values for VA and SA than Langmuir model.

The change of energy involved in sorption process were negative for VA and SA (-34.2 and -13.1 kJ/mol, respectively), indicating that the adsorption was exothermic. The phenolic acids had a similar behaviour as the aldehydes studied by some authors.

Fixed-bed experiments of VA and SA adsorption onto the Sepabeads SP700 were also performed, obtaining the respective breakthroughs. For the VA the essays comprised a feed concentration (C_f) of 1.40 g/L at 288 K and at 313 K and, two C_f of 0.67 g/L and 1.22 g/L at 298 K. For SA the essays comprised a C_f of 0.71 g/L at 288 K and at 313 K and, two C_f of 0.16 g/L and 0.67 g/L at 298 K.

The equilibrium data obtained with the fixed bed studies matched the Freundlich model found with batch adsorption study.

Elution studies with ethanol/water (90/10, v/v) were performed and practically all adsorbed solute was recovered in each essay (adsorption and desorption capacities were similar). Additionally, more than 90 % of adsorbed VA and SA was recovered with five bed volumes of ethanol/water (90/10, v/v), with the exception of VA essay at 288 K, were a recovery of 85 % was achieved.

KEYWORDS: Vanillic acid, syringic acid, batch adsorption, fixed bed, adsorption, capacity of adsorption, Langmuir model, Freundlich model.

Resumo

Os ácidos fenólicos como o ácido vanílico (VA) e seríngico (SA) resultam da oxidação da lenhina com O_2 em meio alcalino, um processo focado principalmente para a produção de vanilina (VL) e seringaldeído (SY). Estudos de separação e recuperação de VA e SA são escassos. No entanto, esses dois ácidos fenólicos têm muitas aplicações na indústria farmacêutica e por isso é importante investigar a sua possível recuperação da mistura oxidante de lenhina. Esta tese teve assim como propósito principal, estudar a adsorção de VA e SA numa resina não-iónica, Sepabeads SP700, visando a sua separação dos outros produtos e recuperação.

Foram realizadas experiências em batch de adsorção de equilíbrio a três temperaturas diferentes (288, 298 e 333 K) para soluções aquosas de VA e SA e os resultados experimentais foram ajustados às isotérmicas de equilíbrio de adsorção dos modelos de Langmuir e Freundlich. Através da aplicação do modelo de Langmuir obteve-se uma capacidade máxima de adsorção de 0.475 g/g para o VA e 0.391 g/g para o SA. Para o modelo de Freundlich obteve-se um 1/n de 0.383 e 0.396 para o VA e o SA, respetivamente, o que indicou que a adsorção foi favorável. Este modelo previu melhor os valores de capacidade de adsorção em equilíbrio obtidos para o VA e o SA.

Os valores de energia envolvida no processo de sorção obtidos para os dois compostos foram negativos (-34.2 e -13.1 kJ/mol), indicando que a adsorção teve um comportamento exotérmico. Os ácidos fenólicos tiveram um comportamento semelhante aos aldeídos estudados por alguns autores.

Foram também realizadas experiências em leito fixo para o VA e o SA com a resina Sepabeads SP700 e foram obtidas as respetivas curvas de rutura. Para os ensaios com VA foi utilizada uma concentração de alimentação (C_f) de 1.40 g/L a 288 K e outra a 313 K e duas C_f de 0.67 g/L e 1.22 g/L a 298 K. Para os ensaios com SA utilizou-se uma C_f de 0.71 g/L para 288 K e outra igual para 313 K e duas C_f de 0.16 g/L e 0.67 g/L para 298 K.
No leito fixo os valores de q_e ajustaram-se ao modelo de Freundlich obtido pelos estudos de adsorção em batch.

Foram realizados estudos de dessorção com etanol/água (90/10, v/v) e praticamente todo o soluto adsorvido foi recuperado em cada experiencia (as capacidades de adsorção e dessorção foram semelhantes). Adicionalmente, foi possível recuperar mais de 90 % de VA e SA adsorvido em 5 volumes de leito de etanol/água (90/10, v/v) com exceção para o VA a 288 K que teve uma recuperação de 85 %.

Palavras-chave: Ácido vanílico, ácido seríngico, adsorção em batch, leito fixo, capacidade de adsorção, modelo de Langmuir, modelo Freundlich.

List of Figures

List of Tables

List of Equations

List of Contents

Nomenclature

A	Cross sectional area of the column	cm^2
C_0	Initial concentration of adsorbate in solution	g/L
C_e	Concentration of the sorbate in the liquid phase at equilibrium	g/L
Cf	Feed concentration in fixed bed experiments	g/L
d_c	Diameter of column	cm
ε_c	Porosity of column	-
fh	Humidity factor of resin	-
ΔH	Change in enthalpy	kJ/mol
i	Number of experiments of 1 to p.	-
K_F	Constant related to the free energy of adsorption for Freundlich	$(g/g) / (L/g)^{1/n}$
K_L	Constant related to the free energy of adsorption for Langmuir	L/g
K	Isotherm constant related to the free energy of adsorption *for Langmuir or Freundlich models	$*L/g$ or $(g/g)/(L/g)^{1/n}$
K^0	Equilibrium constant *for Langmuir or Freundlich models	$*L/g$ or $(g/g)/(L/g)^{1/n}$
L_c	Column length	cm
n	Heterogeneity Factor	-
p	Total number of experimental points	-
ρ_{app}	Apparent density of resin	g wet resin /L resin
q_{max}	Maximum adsorption capacity	$g_{adsorbate} / g_{dry\ adsorbent}$
q_e	Amount of solute adsorbed per weight unit of adsorbent at equilibrium	$g_{adsorbate} / g_{dry\ adsorbent}$
$q_{e,calc}$	Theoretical adsorbed concentration in solid phase at equilibrium	$g_{adsorbate} / g_{dry\ adsorbent}$
$q_{e,means}$	Experimental adsorbed concentration in solid phase at equilibrium	$g_{adsorbate} / g_{dry\ adsorbent}$
q_f	Adsorption capacity for C_f	$g_{adsorbate} / g_{dry\ adsorbent}$

q_{des}	*Desorption capacity*	$g_{adsorbate}/g_{dry\ adsorbent}$
Q	*Flow rate*	*L/min*
R	*Universal gas constant (8.314×10^{-3})*	*kJ/molK*
T	*Absolute temperature*	*K*
t_{st}	*Theoretical stoichiometric time*	*min*
$t_{st,exp}$	*Experimental stoichiometric time*	*min*
u_0	*Superficial velocity*	*cm/min*
u_i	*Interstitial velocity*	*cm/min*
V_0	*Volume of solution*	*L*
V	*Column volume*	*L*
$w_{adsorbent}$	*weight of adsorbent*	*g*

Abbreviations

ERRSQ	*Sum of square of the errors*
SA	*Syringic acid*
SY	*Syringaldehyde*
VA	*Vanillic acid*
VL	*Vanillin*

1 Introduction

1.1 Background and motivation

Portugal has one of the most important pulp and paper industries being the 4th largest European producer of pulp and the 3rd of chemical pulps in 2012.[1] Kraft pulping is one of the processes involved in the pulp and paper production. In this process the delignification of the wood matrix promote the liberation cellulose and a fraction of the original hemicellulose and promoting the lignin dissolution in pulping liquor, resulting in an effluent called black liquor.[2]

Kraft pulping is the main process used in the world for production of pulp for paper. The production of 500 thousand tons of kraft pulp (typical for an average-size mill) corresponds to about 290 thousand tons of the black liquor with a solids content of 15%. About one half of these solids is lignin.[2] Pulping liquor is the main source of lignin easily accessible on large scale and comes from wood delignification in pulp and paper industries. The most part of lignin produced in pulp and paper industries, is mainly used for energy recovery at the pulp mills, and only a small fraction is used for commercial applications, mostly in lignosulfonate form.[3] The separation of lignin from black liquor and the conversion of lignin into high-value products have becoming noticeable in the recent years.[4,5]

In lignocellulosic biorefinaries, cellulose is the main target of the biomass delignification with the goal of producing bioethanol. There are only a few biorefineries which use the lignin to convert into high-value products. Borregaard is one of the most advanced biorefineries. This company is a supplier of lignosulfonate and vanillin (VL) produced from lignin, which is separated during the production of cellulose. In pulp and paper industries, lignin is a by-product exceeding 50 million tons per year.[6]

Lignin is a three-dimensional phenolic macromolecule composed by distinct aromatic nuclei: p-hydroxyphenyl (H), guaiacyl (G), and syringyl nuclei (S). Softwood lignins are G:H type and hardwood lignin are S:G:H type. Thus, kraft operations are highly integrated and depend on black liquor for pulping chemicals recovery and as fuel.

The typical hardwood lignin is a copolymer of coniferyl and sinapyl alcohols (Figure 1) being usually indicated as "guaiacyl-syringyl lignin".[2]

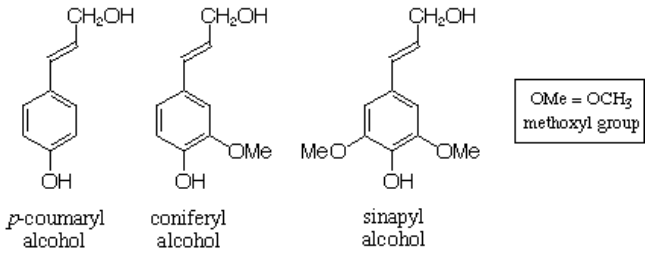

***Figure 1**. The precursors of p-hydroxyphenyl, guaiacyl and syringyl moieties of the lignin structure[2]*

According to the plant material there are different proportions of these monomers. These monomers can establish different linkages leading to a complex molecule.[7]

A representation of a molecular fraction of kraft lignin is shown in figure 2.

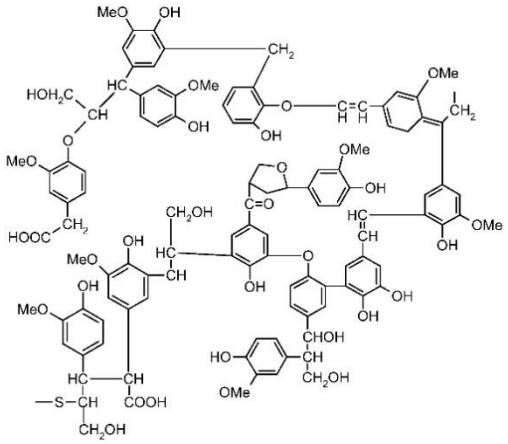

***Figure 2**. A structural model of a technical lignin fragment (kraft lignin)[8]*

The source of biomass in pulp and paper industry and the delignification process have significant interference on the structure of the lignin (linkages and functional groups).[3]

Eucalyptus species represents the main raw-material for the pulp industry in South America, Portugal and Spain. In Portugal, approximately 7 million m^3 of debarked *Eucalyptus globulus* wood per year is used in pulp production for high performance paper.[3]

The oxidation of lignin at specific and controlled conditions produces a complex mixture of phenolic compounds, namely syringaldehyde (SY), vanillin acid (VL), vanillic acid (VA) and syringic acid (SA), as depicted in Figure 3.[2]

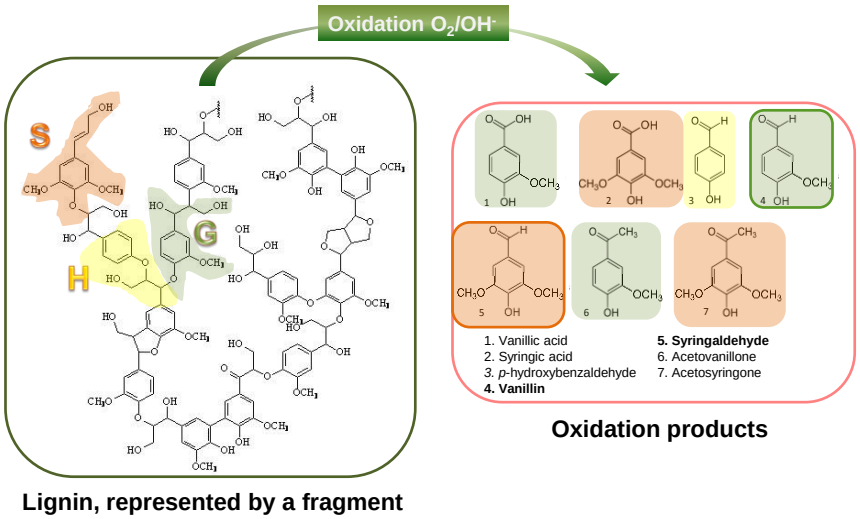

Figure 3**. Mixture of phenolic compounds obtained by oxidation of lignin. **(source: Internal Document LA LSRE-LCM courtesy of Paula Pinto, 2015)

The lignin-rich side streams currently produced in pulp and paper industries and in biorefinaries are mainly derived from hardwoods and annual/perennial plants. As such, besides VL and VA, also syringil-derived compounds (SY, SA, acetosyringone) are produced in the oxidation process of lignin, increasing the complexity of the mixture obtained. Therefore, it is important the study of processes aiming the separation of these final products.

The VA and SA have not been studied as compounds produced from lignin. However, these two phenolic acids compounds have many applications on pharmaceutical industry[9,10] and their possible valorisation needs to be investigated.

Recently, the phenolic acids, such as SA and VA, has had good results in studies of treatments against aging and for a wide variety of diseases, including cancer, Parkinson´s, and chronic inflammatory diseases. This is the reason why the interest on these compounds is increasing.[9, 10] The molecular structure of these two acids is shown in figure 4.

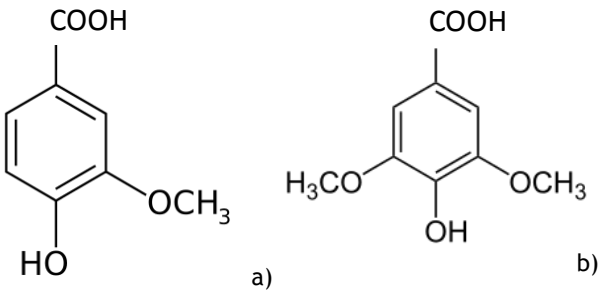

***Figure 4**. Molecular structure of a) vanillic acid (VA) and b) syringic acid (SA)*

When compared to other processes such liquid-liquid extraction, crystallization, distillation, adsorption can be a more suitable process to recover phenolic compounds due to

its relative simplicity of design, operation and scale up. Additionally, adsorption processes it is ease to regenerate and usually has low cost.[11]

1.1.1 Research area 'Lignin Valorisation'

The research area in 'Lignin Valorisation' is included in the topic 'New High Value-Added Products from Agro-Food Resources' within the RG2.

Valorisation of lignin has been one of the key research topics at LSRE. Since 90's a consistent program of reaction and separation processes have been developed for oxidative depolymerisation of lignin, subsequent recovery of high-added value chemicals, and polymers synthesis. This subject has been intensively studied under the leadership of Professor Alírio Rodrigues. The research program started with the process development of VL production from softwood lignin in batch reactor. Later on a structured packed bubble column reactor for continuous production was designed and built leading to the Ph.D Thesis 'Production of VL from Lignin Present in the Kraft Black Liquor of the Pulp and Paper Industry' (2008, José Daniel Pacheco Araújo). Concerning separation, LSRE team studied ultrafiltration and adsorption processes demonstrating its application in the recovery of VL from lignin solutions. In another perspective, although complementary to the first one, the team also developed the production of lignin-based polymers, such as polyurethanes, in collaboration with EFPG, Grenoble.

Recently, the research team has been working on different types of lignin, finding additional high added-value compounds, in the perspective of valorising the side streams from new processes (and raw materials) in biorefineries. Two Ph.D thesis are currently ongoing: 'VL and SY from Side Streams of Pulp & Paper Industries and Biorefineries' (Carina Costa) and 'Fractionation and Purification of SY and VL from Oxidation of Lignin' (Inês Mota). Moreover, the team is also working on two industry-driven projects in the lignin valorisation topic.

The team has been working on adsorption and desorption of VL and SY onto two different macroporous resins. The integrated process is present in figure 5. However, the adsorption and desorption behaviour of VA and SA, two important products resulting from lignin oxidation, was never studied in one of the most promising resins previously found for VL and SY. Therefore, the main contribution of this work is to study the adsorption and desorption of VA and SA from aqueous solutions using the nonpolar resin SP700.

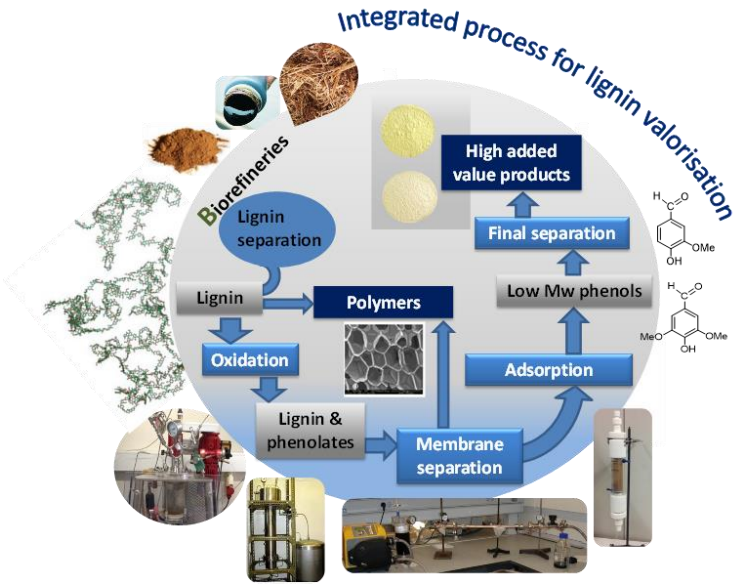

***Figure 5**. Simplified flow sheet of the integrated process for production of value-added functionalized monomers from lignin-and polymers from lignin (source: Internal Document LA LSRE-LCM courtesy Paula Pinto, 2015)*

1.2 Objectives of the work

This dissertation aimed to contribute to the study of VA and SA recovery from the mixture resulting from lignin oxidation as part of a broader project for lignin valorisation in lignocelullosic biorefineries and pulp and paper industries. The main objectives of this work are:

1. To perform equilibrium batch adsorption studies of VA and SA in mono-component aqueous solution onto Sepabeads SP700 for different temperatures;
2. To apply adsorption equilibrium isotherms to describe the adsorption behaviour at different temperatures, evaluating the fitting and resulting parameters, such as adsorbent capacity;
3. To understand the influence of temperature on the adsorption of these phenolic compounds;
4. To perform fixed bed studies at different feed concentrations and temperatures and comparing the results with the data from batch experiments;
5. To perform desorption studies employing 90:10 % V/V ethanol:water solution.

1.3 Research unit presentation

1.3.1 Brief description

The R&D Associate Laboratory LSRE-LCM, a partnership between LSRE (Laboratory of Separation and Reaction Engineering) and LCM (Laboratory of Catalysis and Materials), is a

research unit operating within the Department of Chemical Engineering of Faculty Engineering of the University of Porto, with two external Poles at Instituto Politécnico de Bragança and Institution Politécnico de Leiria. At present, LSRE-LCM integrates a total of 117 researchers, 69 holding a PhD degree and 27 PhD students. There internationally recognized scientific activity is well expressed by over 920 articles published in the 2005-2013. The mission of the LA is to contribute to the scientific and technological development at National and EU levels in the areas of Separation and Reaction Processes in Chemical Engineering. R&D activities are focused on areas such as: Separation Processes; Reaction Engineering; Process Modelling, Simulation and Control; Environmental Engineering; Heterogeneous Catalysis; and Carbon Materials. A wide range of know-how levels is covered by the LA activities, from fundamental research to the development of industrial products and processes. Training of high-competence researchers and technicians through post-graduate and post-doctoral programmes is a major part of the mission of the LA.

1.3.2 Research lines and groups

The LA is scientifically organized in two thematic Research Lines and four Research Groups (Cyclic Separation/Reaction Processes; Product Engineering; Thermodynamics & Environment; Catalysis and Carbon Materials):

Research Line 1 - New Technologies Of Cyclic Separations/Reactions

The vast experiment of LSRE in separation and reaction processes is the main drive for the various research projects in this area, which are complemented by the know-how of LCM in the field of preparation and development of catalysts and adsorbents. This Research Line comprises the Research Groups: RG1. Cyclic Adsorption/Reaction Processes; RG3. Thermodynamics & Environmental Science and Engineering;

Research Line 2 - Synthesis And Formulation of High-Added Value Products

The combined experiments of LSRE and LCM in this area include various projects for conception and production of high-efficiency catalysts and nanostructured materials, the development of innovative processes and the formulation of high-added value products. This Research Line comprises two Research Groups: RG2. Product Engineering; RG4. Catalysis and Materials.

1.4 Outline of the work

Chapter 1 - Introduction

A brief introduction to the topic of VA and SA was made. The importance of finding sustainable solutions for the recovery of these compounds was contextualized. The objectives and contributions of this work were presented as well as the Research Unit where this project was developed.

Chapter 2 - State of the art

In this chapter is made a data collection of the studies from literature applying the adsorption of VA and SA. The principal results and conditions of the studies were described.

Chapter 3 – Adsorption

The description of the compounds was made. The involved mechanisms in adsorption were explained. The adsorption equilibrium isotherms, the selection of the best adsorbent and the kinetics and thermodynamic aspects of adsorption were discussed. Finally, the techniques of adsorption and the equations for calculation of the amount of each compound adsorbed onto the adsorbent (q_f) and desorbed from the adsorbent (q_{des}) were present.

Chapter 4 – Technical description and procedures

The methodology applied to obtain the calibration curve of VA and SA, solubility and stability tests for the two compounds in water and the procedure for adsorption in batch and in fixed bed were explained.

Chapter 5 – Results and discussion

The results obtained in this study were presented and discussed on this chapter, namely the adsorption equilibrium isotherms, and the comparison between the Langmuir and Freundlich models to describe the behaviour of adsorption of the phenolic acids in batch and fixed bed experiments. The effect of temperature on the adsorption capacity was evaluated.

Chapter 6 – Conclusions

The main conclusions of this work were presented in this chapter.

Chapter 7 – Limitations and future work

The limitations that occurred during the experiments and the work that needs to be done in the future to improve the results were presented.

2 State of the art

2.1 Phenolic acids

Phenolic acids differ by the number and position of the hydroxyl groups on the aromatic ring. These compounds may be divided into two groups: hydroxybenzoic acid derivatives, which include *p*-hydroxybenzoic, protocatechuic, gallic acids, VA and SA and hydroxycinnamic acid derivatives, which include *p*-coumaric, caffeic and ferulic acid.

Through oxidation of the lignin present in black liquor, VA and SA are produced among other low molecular weight compounds.[3] In table 1, the properties of VA and SA are summarized.

***Table 1**. Properties of VA and SA in literature*

Compound	M ($g.mol^{-1}$)	T_{melt} (ºC)	T_{boil} (ºC)	d ($g.cm^{-3}$)	pKa (298 K)	Solubility in water ($g.L^{-1}$)
VA	168.15 [12,13]	207-211.5 [12, 14, 15]	353.4 (101.3KPa)[15]	1.351 [16]	Water: pK_{a1} 4.42, pKa_2 9.39 [17]	≈1.53 (298 K)[18]
SA	198.2 [13]	205 – 209 [16]	192-193 (6.7 KPa) [14, 15] 363 (101.3 KPa) [19]	1.335 [19]	Water: pK_{a1} 4.34, pKa2 9.49 [17]	5.8 (298 K)[15]

The separation and purification of phenolic compounds can be achieved by different technologies, adsorption is the most studied.

Studies on adsorption of VA and SA are scarce and limited to the adsorption onto activated carbon.[20, 21-23]

The activated carbon is the most used adsorbent due the great adsorption capacity for organic compounds in industrial applications (purification and recovery in chemical and pharmaceutical processing and environmental remediation). Nevertheless, this adsorbent has high cost, mainly due to an usually expensive regeneration system which make it less economically viable.[24]

The adsorption of the phenolic acids of interest with activated carbon has been studied as well as the influence of some variables such pH and temperature. The main published results are summarized in table 2.

***Table 2**. Studies to recovery VA and SA by adsorption in aqueous solution*

Adsorbate	Adsorbent Characteristics		T (K)	pH	q_{max} (mg/g)	Ref.
	Adsorbent	Surface area (m^2/g)				
VA	AC	1370	293	8*	≈240	[23]
	AC - olive husk derived	≈1000	298	3.2-3.5	148.23 171.46	[22]
	CAC	≈1000	318		56.31 85.10	
SA	AC – bituminous coal	967	293 303 313	3.4-3.7	≈260-320	[21]

(C)AC - (commercial) Activated carbon *pH correct with NaOH and H_2SO_4

The equilibrium adsorption isotherms of SA, from aqueous solutions at 293 K, 303 K and 313 K on a bituminous coal based activated carbon using the batch bottle point method were investigated by Garcia et al.[21] The adsorption isotherms on activated carbon were obtained from the mass balance of dissolved SA. Within the range of temperatures studied (between 293 and 313 K) the temperature did not have a noteworthy influence for equilibrium concentrations until 0.4 g/L: only a slight increase of the adsorption capacity was observed with the temperature rise and thus, results suggested a somewhat endothermic adsorption process. The maximum adsorptive capacity was found for pH range 3-4. For higher pH values there was an important decrease of the adsorption capacity, which was due to the increase of the proportion of the SA ionized form, thus increasing the polarity, resulting in a lower adsorption onto activated carbon.

The adsorption of a mixture of polyphenols (consisting of caffeic acid, VL, VA, *p*-hydroxybenzoic acid and gallic acid) at two temperatures (298 K and 313 K) for different types of activated carbon was studied by Michailof et al.[22] The adsorption isotherms at equilibrium were determined using the batch bottle point method. The adsorption capacity for each compound followed the same trend for the two temperatures: caffeic acid, VL, VA, *p*-hydroxybenzoic acid and gallic acid. The authors have compared the solubility in water of each compound with the adsorption capacity: the lower the solubility, the higher was the adsorption capacity. The observed increase on adsorption with the increase of temperature suggests an endothermic process. To prove the endothermic nature of the adsorption, the authors have studied thermodynamic aspects, $\Delta G°$ and $\Delta H°$. The $\Delta G°$ had negative values ranging between -7.032 and -1.217 kJ/mol, indicating a spontaneous adsorption process. The

authors of this study have stated that the low positive values of ΔH^0, below 20 kJ/mol, indicated physisorption and an endothermic process.

The adsorption of polyfunctional phenols (tyrosol, catechol, veratric acid, VA and caffeic acid) from olive oil mill waste waters on active charcoal at 293 K was studied by Richard et al.[23] The batch bottle point method was one more time applied to obtain the adsorption isotherms. The authors have tried to correlate the adsorption parameters with the structure of the adsorbates but they were not successful. Nevertheless, adsorption capacity for the acidic phenols was much lower than for the other compounds. The Freundlich equation was found to provide the best fit for all the compounds except for the catechol. The main results and conditions are summarized in table 2.

2.2 Phenolic aldehydes

The adsorption and recovery of phenolic aldehydes, such as VL and SY have been more extensively investigated than it was for VA and SA. There are some studies of adsorption with polymeric adsorbents.

Synthetic polymeric adsorbents, such as resins, are durable, chemically inert and stable, and possess high adsorption capacity, efficiency, selectivity and ease of regeneration, with relatively low cost. However, the effective surface areas are smaller than in the case of activated carbon.[11]

Wang et al. investigated the separation of VL and SY from oxygen delignification spent liquor using a non-polar macroporous resin.[25] The authors used the batch bottle point method, studying the effects of pH (4.0 to 6.5), the amount of adsorbent (7.4 to 22.2 g) and the temperature (290 to 330 K). The Langmuir model could describe the isotherm to pH equal to 4.5 and the results demonstrated that the adsorption equilibrium constant decreased with the increasing of pH, which could be explained by the acid dissociation of the compound, whose ionic products are not adsorbed by the resin. The increase of temperature led to a decrease on the adsorption equilibrium capacity, thus, it was concluded that the adsorption process was exothermic, a fact confirmed by the ΔH obtained (-17.68 kJ/mol) for the range of the studied temperatures.

The recovery of dissolved VL from aqueous solutions by adsorption onto three macroporous resins (NKA-2, S-8 and H103) applying the batch bottle point method was studied.[26] The authors have tested the influence of pH and salt concentration on the adsorption capacity for the resin H103. The results demonstrated that the amount of solute adsorbed per weight unit of dy resin at equilibrium (q_e) of the three resins obtained decreased in the following the order: H103, S-8 and NKA-2, what makes sense because the H103 has higher nonpolar surface area. The best q_e was obtained in acid conditions, when the

molecules of VL are neutral. The increase of salt concentration in solution also promotes the *qe* increase. After that, the authors have performed a fixed-bed study, at room temperature with a solution at pH 6.0. The results revealed that the saturated adsorption capacity of VL on H103 resin was 416 mg/g. In desorption studies, the authors obtained more than 96% of the adsorbed VL using five bed volumes of ethanol.

The adsorption of synthetic VL onto non-polar polymeric resin, Sepabeads SP206, using the batch bottle point and the fixed-bed methods was studied by Zabková et al.[27] In batch studies, the results revealed that the increased of temperature between 293 and 333 K have a negative impact on *qe*. The adsorption equilibrium isotherms were described by the Langmuir model. The fixed bed adsorption revealed that the increasing of the temperature led to an early saturation of the bed for both feed concentration of VL (3.30×10^{-3} mol/L and 6.60×10^{-4} mol/L). The same trend was observed with the increase of the flow-rate. The increase of pH in solution led to decrease of the adsorbed VL.

2.3 Resin Sepabeads SP700

The Sepabeads SP700 is an aromatic, non-polar macroporous resin with great adsorption capacity for organic compounds, in particular for polyphenols. There are some studies about the recovery of phenolic compounds by natural sources with very good results of adsorption capacity using the SP700 resin.[28-30] Some examples are depicted in Table 3. The good performance of this resin prompts us to select this as adsorbent for phenolic acids VA and SA.

***Table 3**. Examples of SP700 resin applications for recovery of phenolic compounds extracted from natural sources*

Solution (target phenolic compounds)	Ref.
Grape and wine by-products (phenolics)	[30]
Distilled grape pomace aqueous extracts (phenolics)	[29]
Solvent extracts from auto hydrolysis liquors of grape pomace (phenolics)	[28]

Applications for this resin normally encompass the extraction of antibiotics from fermentation liquors, refinement of pharmaceutical products, polypeptides, proteins, natural extracts (polyphenols) and chromatographic separations of fine chemicals. The application of this resin for the adsorption of derivatives from lignin oxidation, in particular VA and SY is reported in this work for the first time.

3 Theoretical concepts

3.1 Adsorption and adsorption capacity

The adsorption is a process that occurs when a liquid solute (adsorbate) adheres to a surface (adsorbent).

The sorption is the basis of separation of solutes from a mixture due the different proneness to adhere on the sorbent and can be separated in two stages: the adsorption step, where a selective concentration of one or more components is retained on the surface of adsorbent, and the desorption/regenerated step, where the compounds are recovered and the initial adsorbent capacity is restored.

The nature of the bonding between the adsorbate and the adsorbent depends of the species involved and the adsorption phenomenon can be distinguished in physisorption and chemisorption.

The adsorption which results from the influence of van der Waals forces is essentially physical and can be easily reversed. In chemical adsorption there are additional forces that involve the exchange or sharing of electrons, establishing chemical bonds such as hydrogen bonds, π-bonds, acid-base interactions. In this case the process is not so easily reversed, and the regeneration phase could be a problem.[31]

The adsorption capacity of the adsorbent for a specific compound corresponds to the adsorbed amount when concentration reaches a constant value, which corresponds to the equilibrium concentration. Thus, in batch systems the adsorbed amount is given by the difference between the initial concentration and the equilibrium concentration.

The adsorption capacity at adsorption equilibrium, q_e (mg/g of resin), can be calculated by a mass balance given by equation 1.[32]

$$q_e = \frac{(C_0 - C_e) \times V_0}{w_{adsorbent}} \qquad \textit{Equation 1}$$

Where,

C_0 - Initial concentration of solute in solution (g/L);

C_e - Equilibrium concentration of solute in solution (g/L);

V_0 - Volume of solution (L);

$w_{adsorbent}$ - Weight of adsorbent (g).

There are many factors influencing the adsorption capacity such as the nature of the adsorbent and the adsorbate and the solution conditions.

3.2 Selection of adsorbent

The adsorbents have a natural origin or result of an industrial production and/or activation process. Typical natural adsorbents are clay minerals, natural, zeolites, oxides or biopolymers. The adsorbents can be classified into carbonaceous adsorbents, polymeric adsorbent and zeolite molecular sieves. The activated carbon produced from carbonaceous material is the most widely applied adsorbent. Polymeric adsorbents produced by copolymerization of non-polar or weakly polar monomers demonstrate adsorption properties comparable to activated carbon.[33]

The surface area is a key quality parameter of the adsorbents. Engineered adsorbents are typically highly porous materials with surface areas in range between 10^2 and 10^3 m^2/g. The porosity does part of internal surface constituted by the pores walls.[33]

The adsorbent characteristics, such as the surface area, functionality, porosity, broad distribution of particle size, impurities and internal porous structure influence the adsorption's performance.[33]

Non-polar macroporous resins in food and pharmaceutical sectors are very viable since the regeneration of these adsorbents does not required high temperatures and they have low cost and limited existent toxicity.[34]

The Sepabeads SP700 is an aromatic, non-polar macroporous resin with great adsorption capacity for organic compounds, in particular for polyphenols.[11]

3.3 Adsorption equilibrium

To analyse the adsorption separation process is fundamental the study of the most appropriate adsorption equilibrium correlation, which allows a better understanding of the adsorption process.[35]

The adsorption equilibrium correlations allow to predict the adsorption parameters and the quantitative comparison of adsorbent behaviour for varied experimental conditions.[35]

The adsorption equilibrium is established when the adsorbate has been in contact with the adsorbent for a sufficient period of time at a constant temperature and pH. In this moment, the concentration of the adsorbate in the bulk solution creates a dynamic balance with the interface concentration.[35]

3.3.1 Adsorption equilibrium Isotherms

The models of adsorption equilibrium isotherms are crucial for analysis and design of the adsorption process. These isotherms describe the relationship between the amount of sorbate retained on the adsorbent and that remaining in the solution at equilibrium at a fixed temperature and pH.[36]

The different models to describe adsorption equilibrium isotherms have been formulated based in terms of kinetic and thermodynamics considerations.

Several adsorption equilibrium isotherms are presented in literature, such as, linear, Redlich-Peterson, Myers, Nitta, and BET isotherms, but the Langmuir Isotherm and Freundlich ones are the most commonly adsorption equilibrium isotherms used to describe the adsorption equilibrium for phenolic compounds.[37]

3.3.1.1 Langmuir isotherm

The Langmuir isotherm is based on reversible monolayer adsorption onto homogeneous surface, without interactions between adjacent adsorbed molecules.[38]

The maximum of adsorption occurs when the monolayer of surface adsorbent is saturated of molecules adsorbed and graphically it corresponds to a plateau where the concentration of solute in solution is constant with the time.[38]

Considering a liquid-solid adsorption, Langmuir model can be represented by the equation 2.[38]

$$q_e = \frac{q_m \times K_L \times C_e}{1 + K_L \times C_e} \qquad \textit{Equation 2}$$

Where,

q_e - Amount of solute adsorbed per unit weight of adsorbent at equilibrium (g/g $_{adsorbent}$);

K_L - Langmuir constant, parameter which relates to the adsorption energy (L/g).

This equation can be rearranged in linear expressions, such as, for example, equations 3 and 4.

$$\frac{C_e}{q_e} = \frac{1}{q_m \times K_L} + \frac{1}{q_m} \times C_e \qquad \textit{Equation 3}$$

$$\frac{1}{q_e} = \frac{1}{q_m \times K_L} \times \frac{1}{C_e} + \frac{1}{q_m} \qquad \textit{Equation 4}$$

The simple procedure to verify if the fit of Langmuir equation can be applied in experimental data consists plotting $\frac{C_e}{q_e}$ versus C_e or $\frac{1}{q_e}$ versus $\frac{1}{C_e}$. A linear relation is achieved and for example, it is possible to determine the $\frac{1}{q_m}$ and $\frac{1}{q_m \times K_L}$ by the slope and the interception, respectively, considering for equation 3.[32]

3.3.1.2 Freundlich isotherm

The Freundlich model describes a reversible adsorption in an heterogeneous system, characterized by the heterogeneous factor (*n*). This model considers the formation of

multilayers of adsorbed molecules. The Freundlich model is described by the empirical equation 5.[32, 39]

$$q_e = K_F \times (C_e)^{1/n} \quad \textit{Equation 5}$$

Where,

K_F - Freundlich constant, parameter which relates to the adsorption energy $(g/g)/(L/g)^{1/n}$;

$1/n$ - Freundlich factor (dimensionless).

The $1/n$ indicates if the adsorption is favourable and ranges from 0 and 1.[32, 39]

The Freundlich equation predicts a gradually increase of the amount of adsorbed solute per unit of adsorbent weight.

Rearranging the equation for its logarithmic form, the following equation is obtained.

$$Ln(q_e) = Ln(K_F) + \frac{1}{n} \times Ln(C_e) \quad \textit{Equation 6}$$

Plotting $Ln(q_e)$ versus $Ln(C_e)$, enables to be determine K_F and $1/n$ through the interception and the slope values, respectively.[32]

In figure 6, is possible analyse the behaviour difference between the Freundlich model and the Langmuir model.

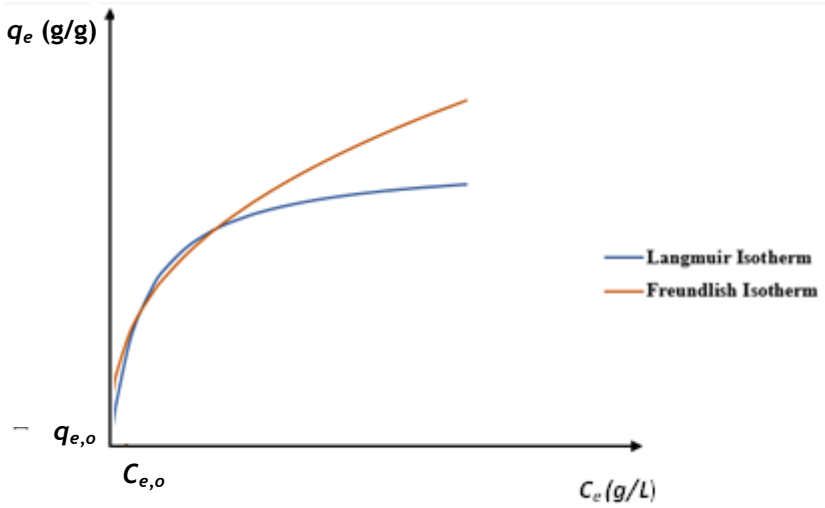

***Figure 6**. Adsorption equilibrium isotherms which follow a behaviour of Langmuir or Freundlich models*

3.3.2 Determination of adsorption equilibrium isotherms

The most commonly approach to determine the adsorption equilibrium isotherm parameters is the linear regression of adsorption equilibrium isotherms.

However, the linear method does not solve the errors in adsorption equilibrium isotherm parameters but it only solves linear forms of equation which measures the difference between experimental data and theoretical data in linear plots, and thus, it has the disadvantage of not providing the best isotherm constants to explain the experimental data obtained. Many studies conclude that the non-linear regression method is the best approach to obtain the isotherm parameters and also to select the best isotherm.[40]

The most common non-linear method is using the error function: the sum of the square of the errors (ERRSQ). This error function gives a best fit with the increasing of the errors, thus higher equilibrium concentrations studied have major contribution for parameters estimation.[36]

$$ERRSQ = \sum_{i=1}^{p} (q_{e,calc} - q_{e,means})_i^2 \quad \textit{Equation 7}$$

Where,

$q_{e,calc}$ – Theoretical adsorbed concentration in solid phase at equilibrium (g compound/g adsorbent);

$q_{e,means}$ – Experimentally adsorbed concentration in solid phase at equilibrium (g compound/g adsorbent);

i - *N*umber of experiments of 1 to *p*.

3.4 Kinetics and thermodynamics of adsorption processes

Adsorption kinetics adsorption describes the time-dependent evolution of the adsorption process until the equilibrium is reached.[32, 41]

The transport in adsorption process can be separated in mass transport and heat transport. The mass transport is divided in 4 stages:

1. Transport of the adsorptive from the fluid phase to the subsurface (built up around the adsorbent);
2. Transport through the subsurface (film diffusion);
3. Simultaneous transport into the pores of the adsorbent through diffusion along the inner surface (surface diffusion);
4. Interaction with the active sites of the adsorbent.

The heat transport is divided into energy transfer inside the adsorbent material and energy through the subsurface surrounding the resin particles.

The thermodynamic parameters are important to understand and predict the behaviour of adsorption of the components in study. Change in Gibbs free energy, enthalpy and entropy are some of the important thermodynamic parameters that are usually calculated.[32, 41]

Arrhenius relationship can be used to determine the change of enthalpy (*ΔH*), Equation 8.[42]

$$K = K^0 \times e^{-\Delta H/RT} \quad \textit{Equation 8}$$

Where,

K^0 - Equilibrium constant (L/mg to calculate K_L or $(g/g)/(L/g)^{1/n}$ to calculate K_F);

R - Universal gas constant (8.314×10^{-3} kJ/mol.K);

T- Absolute temperature (K).

This parameter indicates that the adsorption has an exothermic (negative value) or endothermic nature (positive value). It can also differentiate between physical and chemical adsorption process. In a more detailed way, the type of interactions and the approximate values of energy associated are: van der Waals interactions (4–8 kJ/mol), hydrophobic interactions (4 kJ/mol), direct and induced ion–dipole and dipole–dipole interactions (2–29 kJ/mol), hydrogen bonding (2–40 kJ/mol), charge transfer, ligand-exchange and ion bonding (40 kJ/mol), and chemisorption (covalent bond) (60–80 kJ/mol). The physical sorption processes involve van der waals interactions, interactions between dipole (permanent or induced) moments of sorbate and sorbent molecules and hydrophobic interactions. Chemical interactions involve covalent bond and hydrogen bond.[43]

3.5 Techniques of adsorption

The applications of adsorbent technology and the industrial equipment are highly variable. The most used process and simple technology for adsorption is the batch and the fixed bed processes.[44]

In batch adsorption, a fixed amount of adsorbent is contacted with a defined volume of solution, with agitation, until the adsorption equilibrium. The concentration in solution will decrease with the time until the equilibrium, as described in figure 7.[32]

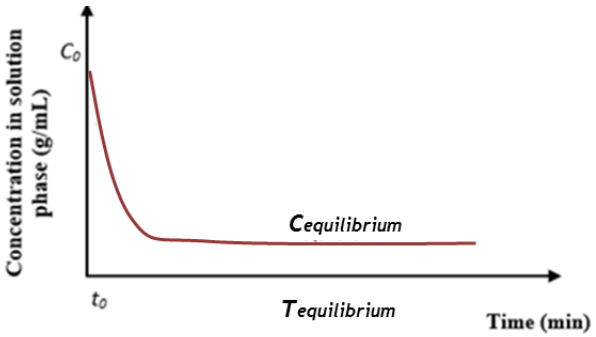

***Figure 7**. Variation of concentration in solution with the time for batch adsorption*

In fixed bed process, the adsorbent bed receives a feed of constant concentration. At beginning, the first layer of the bed, close to the feed, adsorbs the solute present in solution until equilibrium is reached with the incoming fluid. The outlet concentration increases until the equilibrium is reached in the overall bed. This is illustrated in figure 8, where it is represented the increasing of concentration with the time along the column.[45]

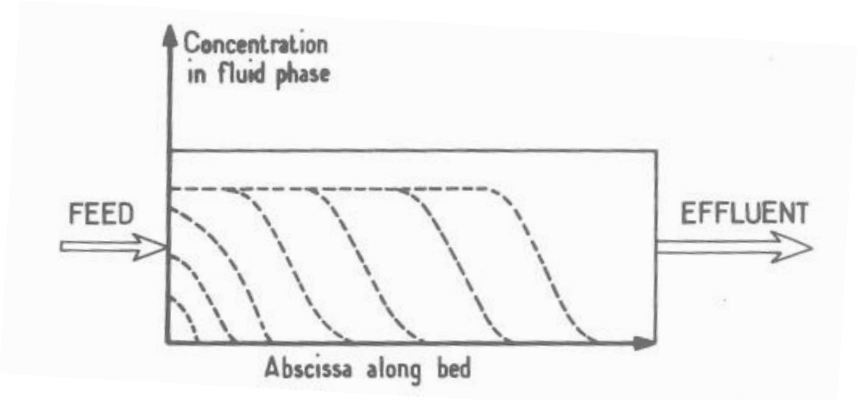

***Figure 8**. Concentration profile at different time in the fixed bed* [45]

The plot of the effluent concentration in the bed with time corresponds to the *breakthrough curve* as depicted in figure 9.[45]

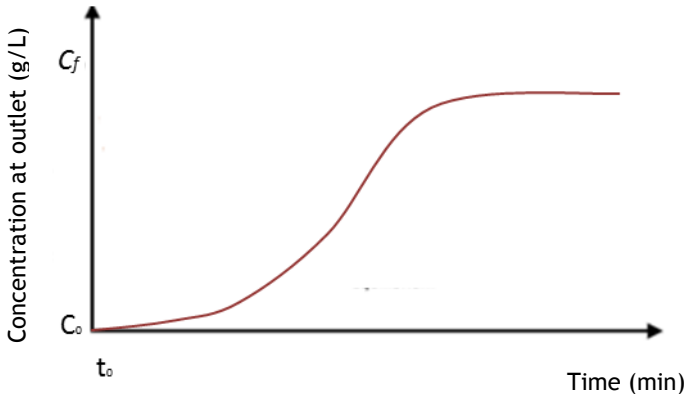

***Figure 9**. Concentration at column outlet* [45]

Analysing the curve, it is visible that in first moments of the process, the concentration of the solute at the outlet is equal or near to zero (C_0, t_0). After that time, the outlet concentration starts growing, until equals the feed concentration (C, t). At this moment, the bed is saturated and can no longer adsorb solute.[45]

The principles and data obtained in batch systems can be used in modelling and designing continuous flow in fixed bed systems.[32]

The superficial velocity, u_0 (m/s) can be calculated by the equation 9, which only considers the flow rate and the column dimensions.[37]

$$u_0 = \frac{Q}{A} \qquad \textit{Equation 9}$$

Where,

Q - Flow rate (mL/min);

A - Cross sectional area of the column (cm^2).

The area is calculated by the form of the column in fixed bed, the most used is a cylinder area, equation 10.

$$A = \frac{\pi}{4} \times d_C^2 \qquad \textit{Equation 10}$$

Where,

d_c - Diameter of fixed bed (cm).

Since the stream of mobile phase flows through of the spaces we can calculate the interstitial velocity, u_i (mL/min), equation 11.[37]

$$u_i = \frac{u_0}{\varepsilon_C} \qquad \textit{Equation 11}$$

Where,

ε_C - Porosity of column.

The theoretical stoichiometric time, t_{st} (min), can be obtained by the equation 12, considering the interstitial velocity.[45]

$$t_{st} = \frac{L_c}{u_i} \times \left[1 + \left(\frac{1-\varepsilon_c}{\varepsilon_c} \right) \times \left(\frac{q_f}{C_f} \right) \right] \qquad \textit{Equation 12}$$

Where,

L_c - column length (cm);

C_f – Concentration of feed flow (g/L).

q_f – adsorption capacity of C_f (g/g $_{dry\ adsorbent}$);

The experimental stoichiometric time, $t_{st,exp}$ (min), during adsorption experiments can be determined by the expression 13.[46]

$$t_{st,\exp} = \int_0^{\infty} \left(1 - \frac{C}{C_f}\right) dt \qquad \textit{Equation 13}$$

Where,

C – Concentration of solution in outline for time t (g/L).

The integral of the last equation is estimated applying the trapezium area for the plot $1\text{-}C/C_0$ vs time.

The experimental stoichiometric time is used to calculate the amount of compound adsorbed by the equations 14 and 15.[46]

- Adsorbed amount:

$$q_{ads} = \frac{Q \times C_f \times t_{st,\exp}}{V \times (1-\varepsilon_C) \times \rho_p (1-fh)} - \frac{\varepsilon_C \times C_f}{(1-\varepsilon_C) \times \rho_p (1-fh)} \qquad \textit{Equation 14}$$

- Desorbed amount:

$$q_{des} = \frac{\int_0^t C dt \times Q}{V \times (1-\varepsilon_C) \times \rho_p (1-fh)} - \frac{\varepsilon_C \times C_f}{(1-\varepsilon_c) \rho_p (1-fh)} \qquad \textit{Equation 15}$$

Where,

ρ_p - Apparent density of adsorbent (g $_{wet\ adsorbent}$ /L $_{adsorbent}$);

fh - Humidity factor of the adsorbent (water/wet adsorbent weight ratio);

V - Column volume (mL).

The theoretical values obtained by the adsorption equilibrium isotherm selected must to be close to the experimental values.

4 Technical description and procedures

4.1 Chemicals and adsorbent

The VA (97%) and SA (98%) were purchased from Aldrich Chemical Company, Inc.

The resin used as sorbent was Sepabeads SP700 (Mitsubishi Chemical Corporation). The main properties provided by the supplier and obtained by characterization at LSRE (Inês Mota) are summarized in Table 4.

***Table 4**. Main properties of the resin SP700*

	Supplier information	Experimental values*
Matrix	Styrene-DVB	
Solid Density	-	1.294 (±0.001) g $_{\text{dry adsorbent}}$/mL $_{\text{dry adsorbent}}$
Apparent density	1.01 g/mL	0.3519 g_{dry} /mL_{dry} 0.3237 g_{dry}/mL_{wet} 1.012 g_{wet}/mL_{wet}
Moisture content	60-70 %	68.2 %
Pore volume	≈2.3 mL/g	2.07 mL pores $_{\text{dry adsorbent}}$/g $_{\text{dry adsorbent}}$ 2.25 mL pores $_{\text{wet adsorbent}}$/g $_{\text{dry adsorbent}}$
Particle size	450 μm	483 μm
Porosity	0.81 (average)	0.728
Specific surface area	1200 m^2/g	-
Average pore radius	90 Å	-

*Values determined by the team in laboratory for the other work

4.2 Equipment

The quantification of VA and SA was performed using a Knauer HPLC system (Knauer, Berlin, Germany) equipped with a Smartline Manager 5000 online degasser, a Smartline quaternary Pump 1000, a column ACE 5 C18-PFP (50×3.0 mm id), and a Smartline UV-Vis Detector 2600, operating at 280 nm. The analytical column used an isocratic elution as eluent (eluent 1: 95% water, 5% methanol and 0.1% acid formic and eluent 2: 95% methanol, 5% water and 0.1% acid formic, 50/50 %, v/v) with a flow rate of 400 µL/min. The pressure was 168 MPa, the temperature 298 K and the volume of injection was 20 µL. The data acquisition was performed using Clarity® version 3.0.6.589.

The batch bottle point experiments were carried out in an orbital shaker SI-300R Lab. Companion. It was used an ultrasounds Starsonic 35 and samples were filtered through a 0.2 µm Nylon membrane. A Smartline quaternary Pump 1000 was used in fixed bed and the temperature was controlled with a thermostatic bath LAUDA RE 206.

4.3 Calibration Curves for HPLC

A mother solution of about 0.3 g/L for each phenolic acid was prepared with methanol and several standards were obtained with different dilutions in eluent 1 (200x, 100x, 50x, 40x and 20x) which corresponded to different concentrations.

Afterwards, calibration curves for each compound were obtained plotting the peak area after injection in the HPLC-UV with the respective concentration. The figure is represented in appendix A.

4.4 Solubility and stability tests

Initially, solubility and stability tests of the VA and SA in water were assessed for different temperatures. The initial concentration for both VA and SA was about 4 g/L.

Solutions were placed in the ultrasounds for about 3 hours while simultaneously heated in order to assure maximum solubilisation. Then, the solutions were cooled down until room temperature (295 K), filtered through 0.2 µm, and analysed in HPLC-UV.

Solubility of VA and SA were also checked for the temperatures 288 K and 298 K by placing the solution in an orbital shaker at the desired temperature, overnight (12- 24 hours) and filtering between the analysis. The results are in the appendix B.

4.5 Batch adsorption experiments using the bottle point method

Solutions of VA and SA were prepared in deionized water (for the required concentration). Before establishing contact between the adsorbate and adsorbent, the solution was ultra-

sonicated, filtered through of a 0.2 µm nylon filter membrane, and the accurate content on VA and SA was assessed by HPLC-UV after an appropriated dilution.

Afterwards, 100 mL of solution of each compound was placed in contact with different weight of SP700 resin in shake-flasks. The flasks were placed in a rotary shaker at 190 RPM, at fixed temperature (288 K, 298 K, or 313 K) and at constant pH of 3.5.

Experiments were taken after 15 minutes, 1 hour, 2 hours, 3 hours, 6 hours and 24 hours of contact time and the concentration in solution was determined by the HPLC.

The adsorption equilibrium isotherms were calculated applying the Langmuir and Freundlich model. The Arrhenius relationship was used to determine K_L and K_F. The *1/n, q_{max}, K_0 and ΔH* parameters were determined by minimizing of ERRQS. For this, the tool of excel "solver GRG non-linear" was applied. The initial values to find the best solution were determined by linearization of Langmuir or Freundlich model and Arrhenius relationship.

4.5.1 Vanillic acid (VA)

The first step was to prepare different initial concentrations (C_o) of VA with deionized water and three resin weights ($w_{wet\ resin}$) to analyse the adsorption of different conditions of solute and resin amounts. The values of C_o and $w_{wet\ resin}$ are presented in table 5 and the respective ratios are summarized in appendix C (tables 23 to 25).

Table 5**. C_0 and resin weight used in batch adsorption for **VA

Temperature	288 K		298 K		313 K	
Experiment	C_0 (g/L)	$w_{wet\ resin}$ (mg)	C_0 (g/L)	$w_{wet\ resin}$ (mg)	C_0 (g/L)	$w_{wet\ resin}$ (mg)
1.1	1.15	267	1.05	253	1.08	258
1.2	1.15	517	1.05	502	1.08	513
1.3	1.15	750	1.05	765	1.08	761
1.4	1.02	264	1.02	289	1.02	266
1.5	1.02	887	1.02	868	1.02	867
1.6	1.02	1071	1.02	1001	1.02	1071
1.7	1.02	1296	1.02	1251	1.02	1326
2.1	2.25	276	2.02	261	2.21	260
2.2	2.25	514	2.02	510	2.21	512
2.3	2.25	750	2.02	751	2.21	767

4.5.2 Syringic acid (SA)

The same procedure was made for the SA but using C_0 lower due to it lower solubility in water. The $w_{wet\ resin}$ and C_0 tested at three temperatures is summarized in table 6. The values of C_o and $w_{wet\ resin}$ *are* depicted in table 5 and the respective ratios are in appendix D (tables 26 to 28).

Table 6**. C_0 and resin weight used in batch adsorption for **SA

Temperature	288 K		298 K		313 K	
Experiment	C_0 (g/L)	$w_{wet\ resin}$ (mg)	C_0 (g/L)	$w_{wet\ resin}$ (mg)	C_0 (g/L)	$w_{wet\ resin}$ (mg)
1.1	0.59	252	0.55	257	0.54	265
1.2	0.59	501	0.55	535	0.54	509
1.3	0.59	759	0.55	754	0.54	769
1.4	0.59	856	0.55	862	0.54	880
1.5	0.59	1007	0.55	1016	0.54	1018
2.1	0.88	254	0.87	259	0.83	252
2.2	0.88	506	0.87	521	0.83	534

4.6 Fixed-bed adsorption method

Initially, the fixed bed column was conditioned with deionized and ultra-sonicated water. A Smartline quaternary Pump 1000 was used to pump the different solutions through the bed of the adsorbent considered. The temperature of the feed solution and the fixed bed was maintained by a thermostatic bath. Three different temperatures were studied, such as the batch method. The solute concentration at the column outlet was determined by HPLC-UV in the same conditions used for the batch method.

Each experiment can be divided into three stages. The 1st one is the adsorption of the compound (VA or SA) until complete saturation of the bed; in the 2nd stage the adsorbed compounds are recovered with a 90:10 %V/V ethanol:water solution and finally, the 3rd stage encompasses the column regeneration with a 0.1 M $NaHCO_3$ solution and rinsing with deionized water.

To start the experiment, the theoretical stoichiometric time was calculated to predict the duration of each run and the volume of adsorbate solution that will be needed. The time to collect samples was chosen based on these values

Next, the different solutions needed for the three stages previously described were prepared: the adsorbate solution with the defined concentration, the eluent solution (90:10

%V/V ethanol:water), 0.1 M $NaHCO_3$ for regeneration and deionized water (≈2-3 L) to wash the column and recover the initial pH. All these solutions were filtered with a 0.2 μm membrane and ultra-sonicated to remove the air dissolved in solutions.

The feed concentrations (C_f) of VA and SA chosen for fixed bed adsorption were based on the batch results to obtain results in the same range analysed and are depicted in Table 7.

***Table 7**. Cf of VA and SA used in fixed-bed*

Phenolic acid	C_f *at 288 K (g/L)*	C_f *at 298 K (g/L)*	C_f *at 313 K (g/L)*
SA	0.71	0.67	0.71
		0.16	
VA	1.40	1.22	1.39
		0.67	

Each desorption process was made after the adsorbent bed was saturated with each feed solution, and thus, the concentration of solution in outlet of the fixed bed was equal to the feed solution. In the saturation zone samples were taken in thirty minutes interval.

5 Results and discussion

5.1 Batch adsorption experiments using the bottle point method

5.1.1 Time to equilibrium and solute adsorbed per weight unit of adsorbent at equilibrium (*qe*)

The VA and SA adsorption behaviour over time (up to 24 hours) was studied by taking samples at defined time intervals, thus enabling the variation of the contact time between adsorbent and adsorbed for a fixed temperature. The representation of the concentration of VA and SA in solution during the contact time with the adsorbent is in appendixes F and G, respectively (figures 29 to 34).

For the three temperatures it was noticeable a decrease of VA and SA concentration over time particularly for the lowest concentrations and for experiments with higher amount of resin. Furthermore, it is noticeable a higher decrease of SA concentration than that observed for VA. For the three temperatures the concentration at equilibrium (C_e) was attained after 6 hours of contact time.

Therefore, the values of concentration in solution after 6 hours where considered as the equilibrium concentrations and they was used to calculate the amount of solute adsorbed per weight unit of adsorbent at equilibrium (q_e) applying the equation 1 and considering a humidity factor (*fh*) of 68%.

An example of calculation of q_e is presented for the experiment 1.1 of VA at 298 K:

$$q_e = \frac{(C_0 - C_e) \times V_0}{w_{\text{wet adsorbent}} \times (1 - fh)} = \frac{(1.05 - 0.86) \times 0.1}{0.253 \times 0.32} = 0.24 \text{ g VA / g}_{\text{dry resin}}$$

Thus, the q_e was 0.24 g/g for an equilibrium concentration of 0.86 g/L in solution with a C_0 of 1.05 g/L and a resin weight of 0.253 g.

Tables 8 and 9 presents the C_e and q_e values obtained for VA and SA, respectively, for each temperature.

***Table 8**. Values of Ce and qe obtained for VA at 288, 298 and 313 K in batch adsorption*

Temperature	288 K		298 K		313 K	
Experiment	C_e (g/L)	q_e (g/g)	C_e (g/L)	q_e (g/g)	C_e (g/L)	q_e (g(g)
1.1	0.87	0.33	0.86	0.24	0.930	0.19
1.2	0.66	0.31	0.66	0.23	0.798	0.18
1.3	0.54	0.26	0.47	0.23	0.678	0.17
1.4	0.76	0.32	0.79	0.24	0.862	0.19
1.5	0.38	0.23	0.44	0.25	0.540	0.18
1.6	0.32	0.21	0.38	0.23	0.469	0.17
1.7	0.26	0.19	0.32	0.26	0.384	0.15
2.1	1.86	0.46	1.74	0.35	1.972	0.29
2.2	1.62	0.40	1.53	0.31	1.770	0.28
2.3	1.40	0.36	1.29	0.31	1.599	0.26

***Table 9**. Values of Ce and qe obtained for SA at 288, 298 and 313 K in batch adsorption*

Temperature	288 K		298 K		313 K	
Experiment	C_e (g/L)	q_e (g/g)	C_e (g/L)	q_e (g/g)	C_e (g/L)	q_e (g(g)
1.1	0.36	0.28	0.37	0.23	0.365	0.22
1.2	0.24	0.22	0.23	0.19	0.245	0.19
1.3	0.14	0.19	0.16	0.17	0.145	0.17
1.4	0.11	0.18	0.13	0.16	0.115	0.16
1.5	0.10	0.16	0.11	0.14	0.103	0.14
2.1	0.62	0.33	0.62	0.31	0.620	0.26
2.2	0.43	0.29	0.45	0.26	0.434	0.24

The values of C_e and q_e (table 8 and 9) were used to determine the adsorption equilibrium isotherms to each compound and to fit the q_e values to the Langmuir and Freundlich models.

5.1.2 Adsorption equilibrium isotherms

The fitting of q_e values to the Langmuir model were obtained applying the equation 2. The Arrhenius type relationship was used to determine the K_L, equation 9. An example of calculation for experiment 1.1 of VA at 288 K is as follows:

$$K_L = K^0 \times e^{-\Delta H/RT} = 1.63 \times 10^{-6} \times e^{34.2/(8.314 \times 10^{-3} \times 288)} = 2.61 \text{ L/g}$$

Thus, for a ΔH and a K^0 equal to -34.2 kJ/mol and 1.63×10^{-6} L/mol, respectively, it was obtained a K_L of 2.61 L/g at 288 K. Next, it was already possible calculate the q_e value:

$$q_e = \frac{q_m \times K_L \times C_e}{1 + K_L \times C_e} = \frac{0.475 \times 2.61 \times 0.874}{1 + 2.61 \times 0.874} = 0.33 \text{ g/g}_{\text{dry resin}}$$

The q_e was 0.33 $g/g_{\text{dry resin}}$ for a q_{max} of 0.475 $g/g_{\text{dry resin}}$. The isotherm parameters, K^0, ΔH and q_{max} were determined by least-squares fitting of the data through minimizing the sum of the squared residuals between the experimental data points and the estimated values obtained by the Langmuir model and using the tool of the excel 'solver GRG non-linear'. The initial values of K^0, ΔH and q_{max} (input for iterations) to find the best solution were determined by linearization of Langmuir model and Arrhenius equation for each temperature. All the parameters (K_L, K^0, ΔH and q_{max}) for VA and SA are presented in table 10.

***Table 10**. Values of q_{max}, K_L, K^0 and ΔH obtained by fitting to the Langmuir model*

Compound	Temperature (K)	q_{max} (g/g $_{\text{dry resin}}$)	K_L (L/g)	K^0 (L/g)	ΔH (kJ/mol)
VA	288	0.475	2.61	1.63×10^{-6}	-34.2
	298		1.62		
	313		0.83		
SA	288	0.391	6.33	2.67×10^{-2}	-13.1
	298		5.27		
	313		4.09		

Analysing table 10, the enthalpy values were negative demonstrating that the adsorption was exothermic. This is also shown by the k_L decrease with the increase of temperature.

The ΔH values achieved by application of Langmuir model and Arrhenius relationship describes the energy involved in sorption process. It is notorious that VA adsorption is a considerably more exothermic process than SA adsorption, suggesting that the two compounds could be separated by adsorption onto Sepabeads 700.

The q_e and C_e *values* and the fitting of q_e values to the Langmuir model, corresponding to the VA and o the SA adsorption onto Sepabeads SP700 for each temperature considered, are shown in Figure 10 and 11, respectively.

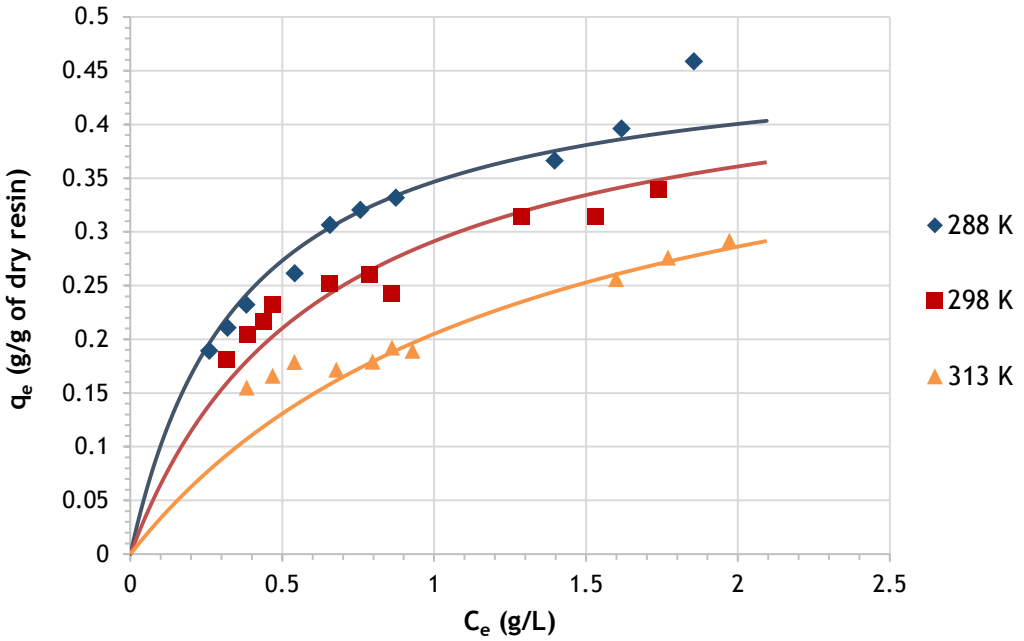

***Figure 10**. Experimental adsorption equilibrium (symbols), qe versus Ce, and fittings to the Langmuir model (lines) at different temperatures (288 K, 298 K and 313 K) for the adsorption of VA onto Sepabeads SP700.*

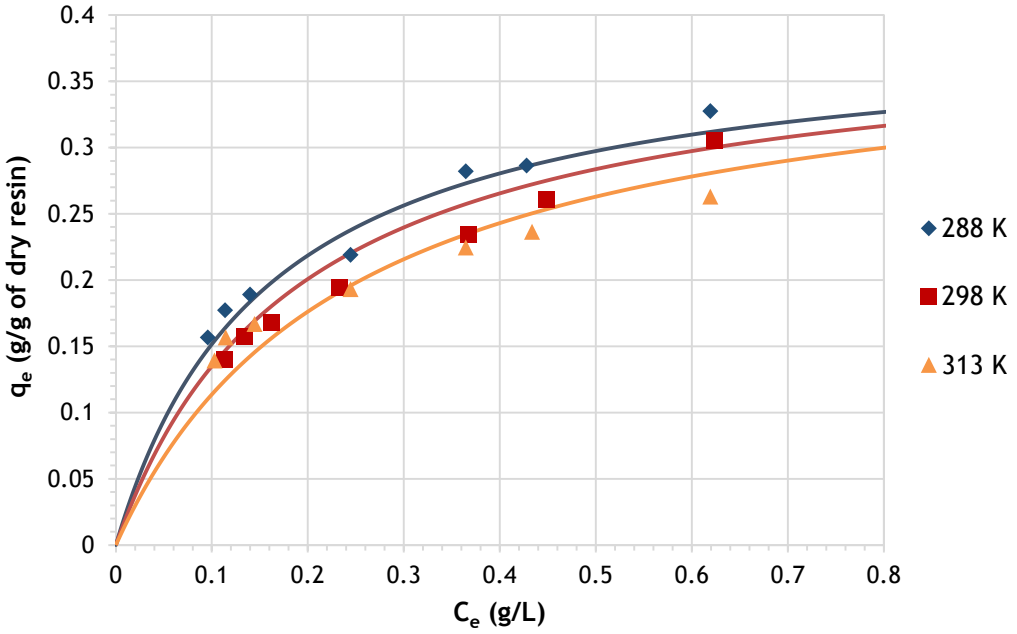

***Figure 11**. Experimental adsorption equilibrium (symbols), qe versus Ce, and fittings to the Langmuir model (lines) at different temperatures (283, 298 and 313 K) for the adsorption of SA onto Sepabeads SP700.*

Observing the figure 10, the increase of temperature promotes the q_e decrease what prove the negative values of ΔH. However, some authors observed the opposite behaviour (endothermic nature) using others adsorbents (such as the activated carbon). Moreover, the

q_{max} values obtained with activated carbon are lower than those obtained applying the macroporous resin Sepabeads SP700.[21, 22] Therefore, the nature (exothermic or endothermic) of VA adsorption depends of the type of adsorbent used. Studies made with VL and SY with non-polar macroporous resin suggests, also, an exothermic behaviour.[25, 27]

For the SA adsorption (figure 11), it was observed that below equilibrium concentrations of about 0.2 g/L, the equilibrium adsorption capacity was not affected by temperature change. For higher concentrations the equilibrium adsorption capacity decreased with the increase of temperature what also proves the negative values of *ΔH* and the exothermic nature of the adsorption. The magnitude of the temperature effect on VA was significantly higher than for SA.

The equation 5 was applied to fitting the q_e values to the Freundlich model. In this case the Arrhenius type relationship was used to determine the K_F, equations 9. An example of calculation for experiment 1.1 of VA at 288 K is as follows:

$$K = K^0 \times e^{-\Delta H/RT} = 9.55\times10^{-4} \times e^{14.08/8.314\times10^{-3}\times288} = 0.34(g/g)/(L/g)^{1/n}$$

Thus, for a *ΔH* and a K^0 equal to -14.08 kJ/mol and 9.55×10^{-4} $(g/g)/(L/g)^{1/n}$, respectively, it was obtained a K_F of 0.34 $(g/g)/(L/g)^{1/n}$ at 288 K, and it was possible calculate the q_e value:

$$q_e = K_F \times (C_e)^{1/n} = 0.34 \times (0.87)^{0.383} = 0.32 \text{ g/g}_{\text{dry resin}}$$

Thus, for a K_F of 0.34 L/g and a *1/n* of 0.383, the q_e obtained was 0.32 $g/g_{\ dry\ resin}$.

The isotherm parameters, K^0, *ΔH* and *1/n* were also determined by application of equation 6 and using the tool of the excel 'solver GRG non-linear'. The initial values of K^0, *ΔH* and *1/n* (input for iterations) and to find the best solution were determined by linearization of Freundlich model and Arrhenius equation to each temperature. All the parameters (K_F, K^0, *ΔH* and *1/n*) for VA and SA are presented in table 11.

Table 11. Values of 1/n, K_F, K^0 and ΔH obtained by fitting to the Freundlich model

Compound	Temperature (K)	1/n	K_f $(g/g)/(g/L)^{1/n}$	K^0 $(g/g)/(g/L)^{1/n}$	ΔH (kJ/mol)
VA	288	0.383	0.34	9.55×10^{-4}	-14.08
	298		0.28		
	313		0.21		
SA	288	0.396	0.39	3.78×10^{-2}	-5.6
	298		0.37		
	313		0.33		

Table 11 shows that the enthalpy values were negative for Freundlich model, as it was for Langmuir model. This proves an exothermic behaviour of adsorption to these compounds. This is also shown by the K_F decrease with the increase of temperature. The ΔH values obtained from Freundlich model are significantly lower than those from Langmuir model. However, the former includes the n (heterogeneous factor), a parameter subjacent to the Freundlich model. The values of 1/n were less than 1 indicating that the adsorption process is favourable.

The q_e and C_e *values* and the fitting of q_e values to the Freundlich model, corresponding to the VA and SA adsorption onto Sepabeads SP700 for each temperature considered, are shown in Figures 12 and 13, respectively.

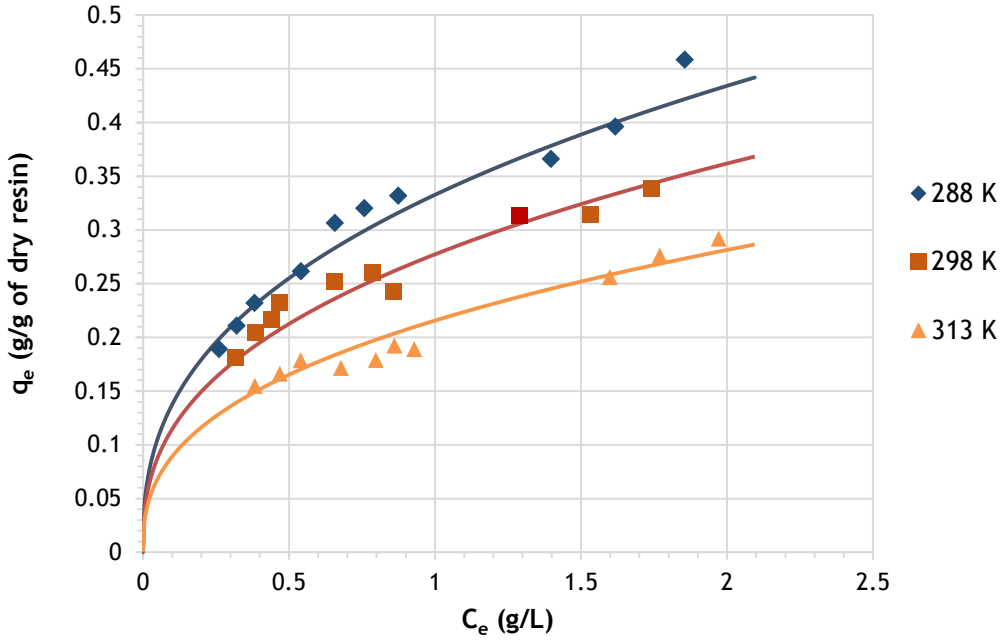

***Figure 12**. Experimental adsorption equilibrium (symbols), q_e versus C_e, and fittings to the Freundlich model (lines) at different temperatures (288 K, 298 K and 313 K) for the adsorption of VA onto Sepabeads SP700*

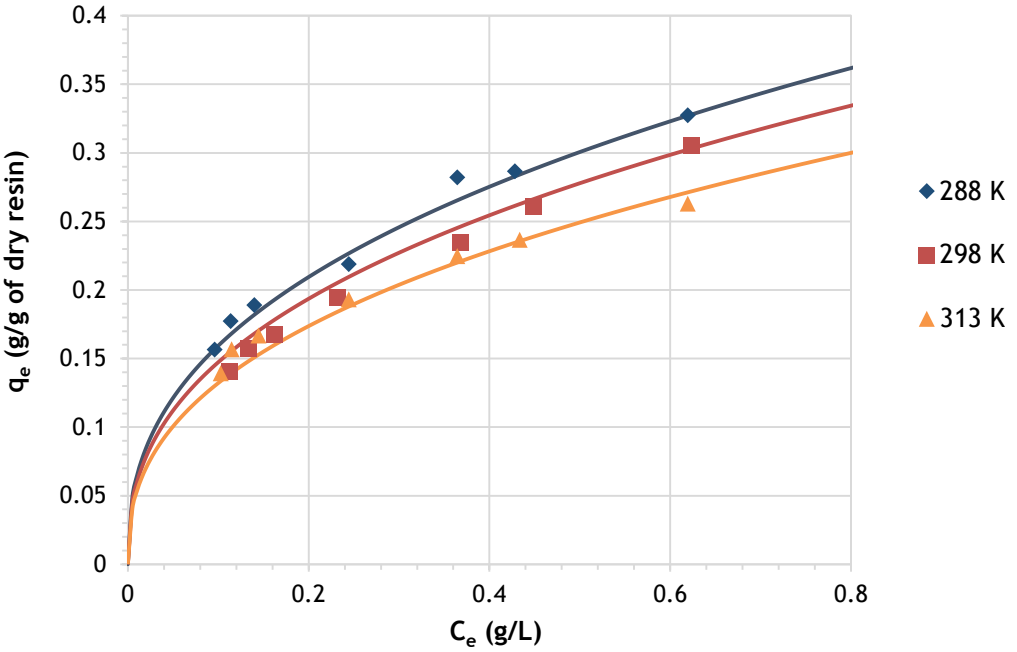

***Figure 13**. Experimental adsorption equilibrium (symbols), q_e versus C_e, and fittings to the Freundlich model (lines) at different temperatures (288 K, 298 K and 313 K) for adsorption of SA onto Sepabeads SP700*

The figures 12 and 13, suggest that the Freundlich model describes better the adsorption behaviour of the two compounds.

The figures 14 and 15 represent the Langmuir and Freundlich models and the experimental data (q_e and C_e) of VA and SA, respectively.

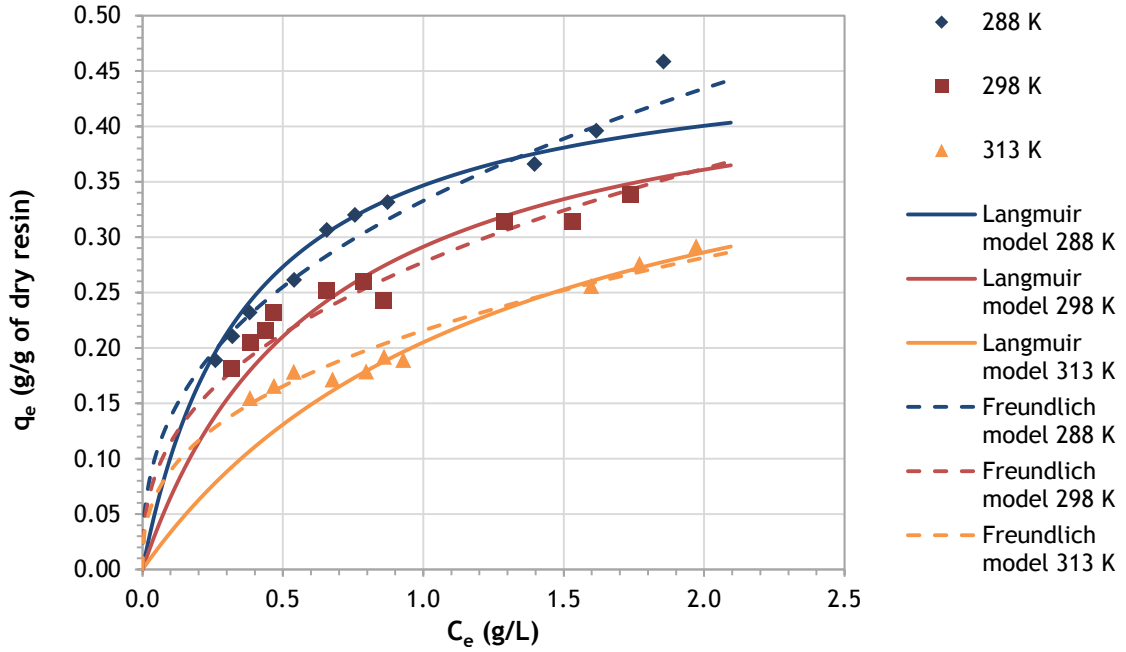

***Figure 14**. Experimental adsorption equilibrium (symbols), q_e versus C_e, and fittings to the Langmuir and Freundlich models (lines) at different temperatures (288 K, 298 K and 313 K) for the adsorption of VA onto Sepabeads SP700*

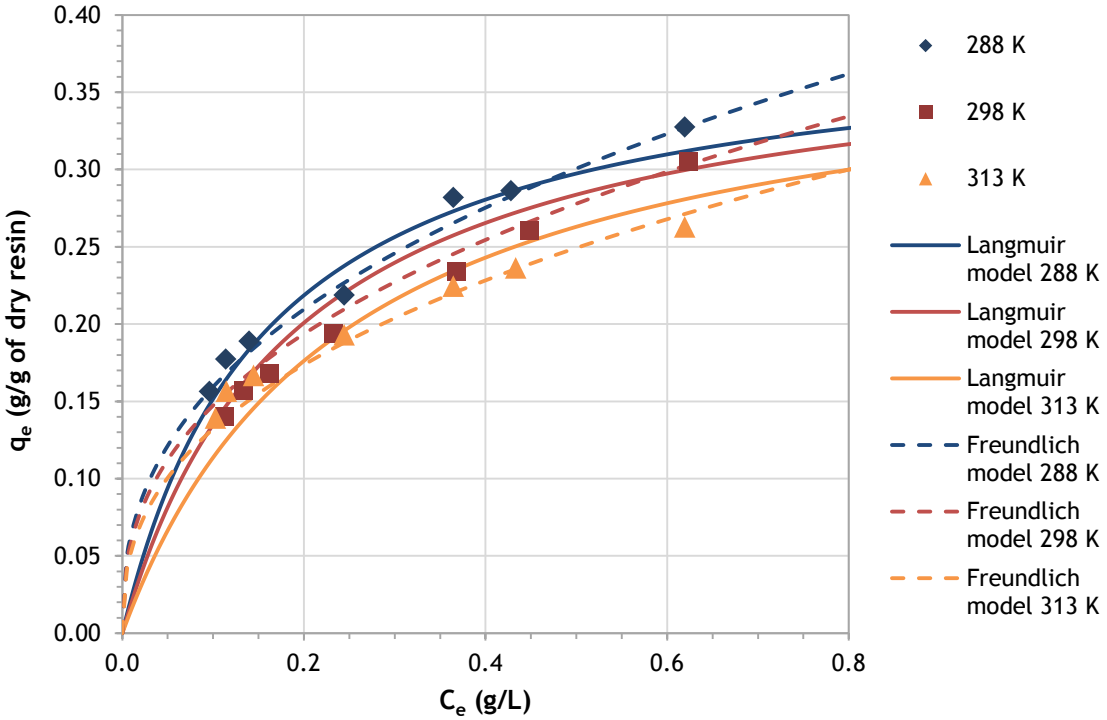

***Figure 15**. Experimental adsorption equilibrium (symbols), q_e versus C_e, and fittings to the Langmuir and Freundlich models (lines) at different temperatures (288 K, 298 K and 313 K) for the adsorption of SA onto Sepabeads SP700*

Observing these figures, the Freundlich adsorption equilibrium isotherms gave a better fitting to the experimental results obtained for VA and SA. Correspondingly the ERRQS values (Appendix E, tables 29 to 32) were also lower for the Freundlich model.
For VA this behaviour is more notorious for C_e bellow 0.5 g/L and for SA mainly for C_e higher than 0.4 g/L.

Richards et al.[23] concluded also that Freundlich model provided a better fitting for VA adsorption onto active charcoal at 293 K. However for VL adsorption onto activated carbon, Wang et al.[25] and Zabkova et al.[27] verified that the Langmuir model provide a better fitting to the experimental results. Although some studies performed with other phenolic compounds onto non polar polymeric adsorbents, similar to SP700, selecting the Freundlich model as the most suitable one.[47]

The adsorption behaviour of SA revealed a better fitting to the Freundlich model than VA. It is also observed that the results of VA had more influence of temperature.

5.2 Fixed-bed adsorption

Cycles of adsorption and desorption for VA and for SA were carried out in the fixed bed to the two compounds. For these experiments, the concentration of the feed (C_f) was selected based on the adsorption equilibrium isotherms at the three temperatures already used for batch adsorption.

The first step, was to calculate the t_{st}, applying the equation 14. The flow rate (Q) used was 5.2 mL/min and the cross sectional area of the column (A) was 0.785 cm^2 which was determine by column diameter (1 cm) and length (5.6 cm) applying the equation 12.

The bed porosity of 0.35 was previously determined by the team with tracer experiments with blue dextran. The interstitial velocity was calculated by the equation 13, obtaining 19.09 cm/min. The adsorption capacity (q_f) was determined by the Langmuir and Freundlich model (equation 2 and 5, respectively) with the parameters determined in batch adsorption. The apparent density of resin (ρ_{ap}) g (wet resin)/L (wet resin) and the humidity factor (fh) were used to convert the units of *adsorption capacity* (q_f) *of* g (adsorbate) /g (dry resin) to g (adsorbate)/L (resin).

An example of calculation is present for VA with a C_f of 0.67 g/L at 298 K applying the Langmuir model:

$$q_f = \frac{q_m \times K_L \times C_f}{1 + K_L \times C_f} \times \rho_{app} \times (1 - fh) = \frac{0.475 \times 1.62 \times 0.67}{1 + 1.62 \times 0.67} \times 1012 \times 0.32 = 80.1\ g/L$$

$$t_{st} = \frac{L_c}{u_i} \times \left[1 + \left(\frac{1 - \varepsilon_c}{\varepsilon_c} \right) \times \left(\frac{q_f}{C_f} \right) \right] = \frac{5.6}{19.09} \times \left[1 + \left(\frac{1 - 0.35}{0.35} \right) \times \left(\frac{80.1}{0.67} \right) \right] = 65.4\ min$$

Thus, at 298 K for a C_f of 0.67 g/L, it was obtained a t_{st} of 65.4 min applying the Langmuir model.

Next, it is presented the calculation of q_f and t_{st} applying the Freundlich model:

$$q_f = K_F \times (C_f)^{1/n} \times \rho_{app} \times (1 - fh) = 0.28 \times (0.67)^{0.383} \times 1012 \times 0.32 = 77.9\ g/L$$

$$t_{st} = \frac{L_c}{u_i} \times \left[1 + \left(\frac{1 - \varepsilon_c}{\varepsilon_c} \right) \times \left(\frac{q_f}{C_f} \right) \right] = \frac{5.6}{19.09} \times \left[1 + \left(\frac{1 - 0.35}{0.35} \right) \times \left(\frac{77.9}{0.67} \right) \right] = 62.9\ min$$

At 298 K for a C_f of 0.67 g/L, it was obtained a t_{st} of 62.9 min applying the Freundlich model.

The C_f, the q_f and t_{st} values obtained applying the Langmuir model and the Freundlich model for VA are in table 12.

***Table 12**. Adsorption capacity and theoretical stoichiometric time for VA applying the Langmuir and Freundlich models*

Experimental conditions	C_f (mg/mL)	1.40	0.67	1.22	1.39
	Temperature (K)	288	298	298	313
Langmuir model	q_f (g/L)	122	80.1	102	79.0
	t_{st} (min)	47.6	65.4	45.4	31.2
Freundlich model	q_f (g/L)	123	77.9	97.1	79.3
	t_{st} (min)	48.0	62.9	43.5	31.3

Table 13 presents the C_f, q_f and t_{st} values obtained applying the Langmuir and the Freundlich models for SA.

***Table 13**. Adsorption capacity and theoretical stoichiometric time for SA applying the Langmuir and Freundlich models*

Experimental Conditions	C_f (mg/mL)	0.71	0.16	0.67	0.71
	Temperature (K)	288	298	298	313
Langmuir model	q_f (g/L)	102	58.0	98.8	88.0
	t_{st} (min)	78.5	197	80.6	67.8
Freundlich model	q_f (g/L)	112	57.5	101	93.3
	t_{st} (min)	85.8	196	82.6	74.4

Analysing the table 12 and 13 it is observed that the theoretical times calculated by each model are not much different. The effect of temperature on adsorption of VA in fixed-bed experiments is show in Figure 16.

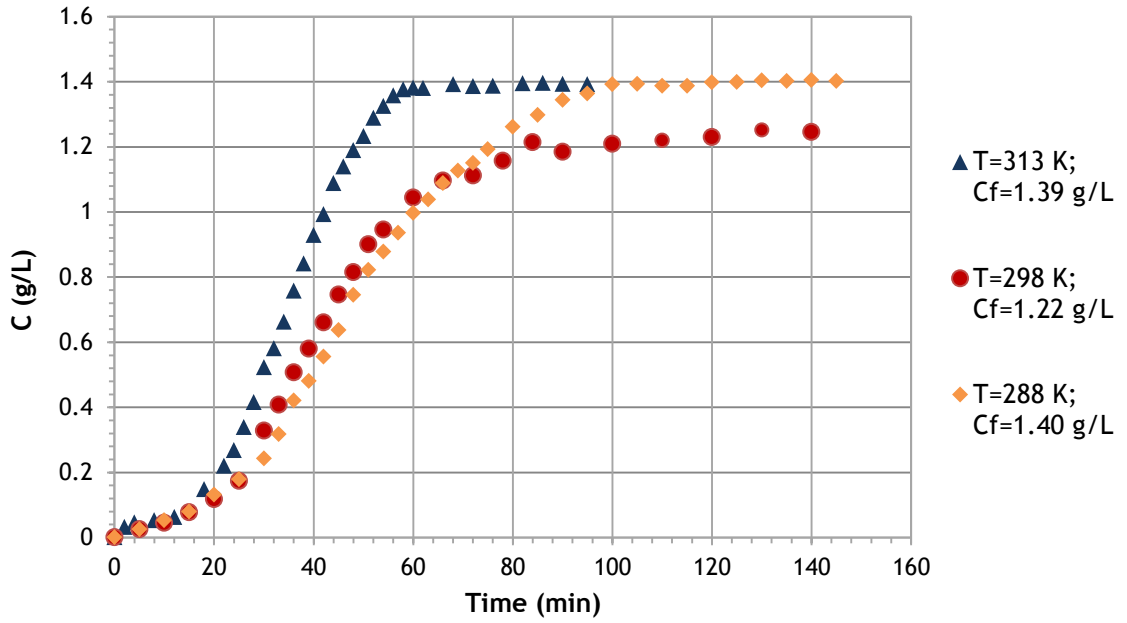

***Figure 16**. Effect of temperature on the fixed bed adsorption of VA onto Sepabeads SP700. Feed concentrations of 1.40, 1.22 and 1.39 g/L at 288, 298 and 313 K, respectively, with flow-rate 5.2 mL/min were tested*

In this case, the adsorption capacity of the bed decreases with the increase of temperature, i.e., the adsorption is favoured by lowering temperature, as it was observed before for the batch experiments. The effect of C_f on VA adsorption in fixed-bed experiments is show in Figure 17.

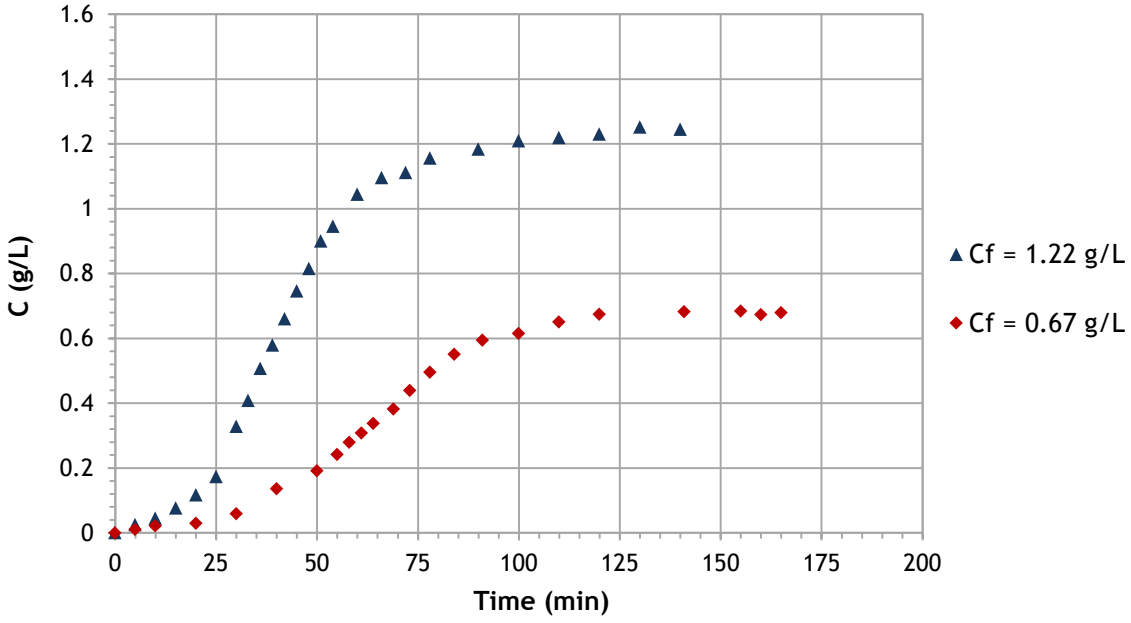

***Figure 17**. Effect of C_f on the fixed bed adsorption of VA onto Sepabeads SP700. The solution was tested for two feed concentrations (0.67 g/L and 1.22 g/L) at 298 K with a flow-rate of 5.2 mL/min*

Comparing the different breakthroughs, it is possible to observe that the time necessary for the bed saturation is lower for the solution with the higher concentration. This is also

observed by the stoichiometric time which is minor for the higher concentration which is expected because a lower feed concentration required more time to reach the bed saturation.

The performance of fixed bed adsorption of SA with the resin SP700 as adsorbent to the temperatures in study (288, 298 313 K) can be seen in Figure 18.

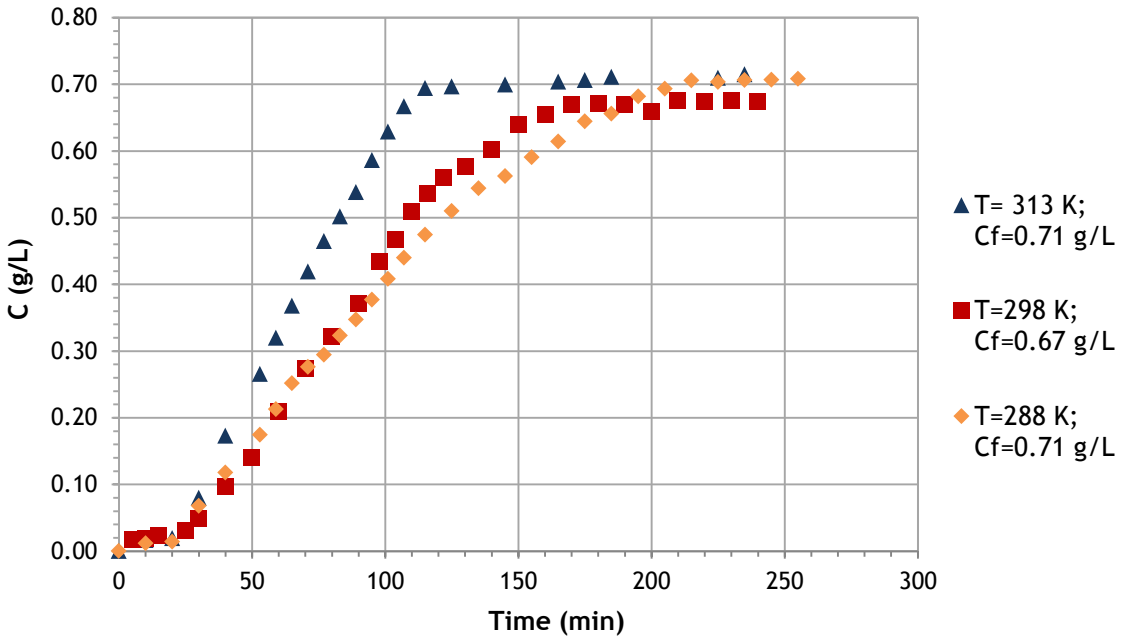

***Figure 18**. Effect of temperature on the fixed bed adsorption of SA onto Sepabeads SP700. Feed concentrations 0.71, 0.67 and 0.71 g/L at 288, 298 and 313 K, respectively with flow-rate 5.2 mL/min were tested*

As already referred for VA, observing the figure 17, the adsorption capacity of the bed decreases with the increase of temperature. If the saturation of column is earlier indicates less adsorption capacity. This is according with the batch experiments because the increase of temperature promotes a decrease of capacity of adsorption in both cases.

The effect of feed concentration on adsorption of SA in fixed-bed experiments is show in Figure 19.

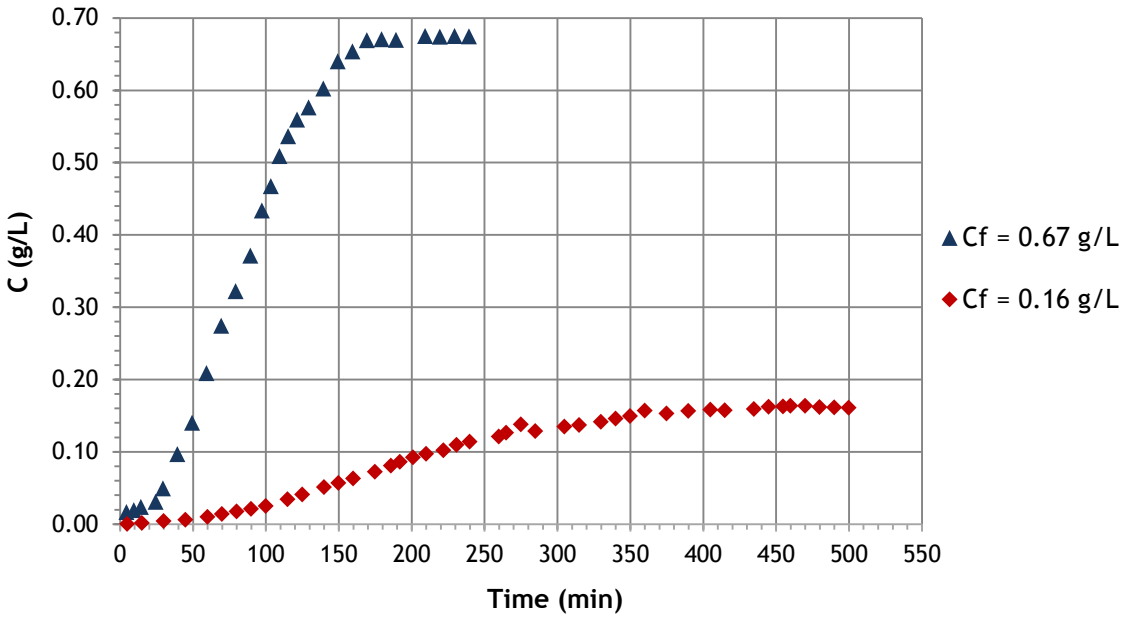

***Figure 19**. Effect of C_f on the fixed bed adsorption of SA onto Sepabeads SP700. The solution was tested to two initial concentrations (0.16 g/L and 0.67 g/L) at 298 K with a flow-rate of 5.2 mL/min*

Observing the figure 19, the t_{st} is the double to the lower concentration of feed stream.

The next stage was to calculate the experimental stoichiometric time. The results obtained for the three temperatures and the difference in relation to the theoretical stoichiometric time obtained (Δt) to the Langmuir and to the Freundlich model for the VA are in Table 14.

***Table 14**. Theoretical and experimental stoichiometric time applying the Langmuir and Freundlich models for VA*

		Temperature (K)			
		288	298	298	313
	C_f (mg/mL)	1.40	0.67	1.22	1.39
Experimental	t_{se} (min)	48.7	62.2	41.9	33.5
Langmuir model	t_{st} (min)	47.6	65.4	45.4	31.2
	Δt (min)	1.12	3.2	3.6	2.3
Freundlich model	t_{st} (min)	48.0	62.9	43.5	31.3
	Δt(min)	0.7	0.7	1.6	2.2

The same procedure was made for SA. The results obtained for the three temperatures and the difference in relation to the theoretical stoichiometric time obtained to the Langmuir and to the Freundlich model are in Table 15.

***Table 15**. Theoretical and experimental stoichiometric time applying the Langmuir and Freundlich models for SA*

		Temperature (K)			
		288	***298***	**298**	**313**
	C_f *(mg/mL)*	0.71	0.16	0.67	0.71
Experimental	t_{se} *(min)*	85.8	193	83.8	73.4
Langmuir model	t_{st} *(min)*	78.5	197	80.6	67.8
	Δt(min)	7.3	4.0	3.2	5.2
Freundlich model	t_{st} *(min)*	85.8	196	82.6	74.4
	Δt (min)	0	3.0	1.2	1

The t_{se} is given by the area obtained by the plots 1-C/C_0 versus time.

The Langmuir model did not satisfactorily predicted the behaviour of the compounds because it gave theoretical stoichiometric times considerably different from the experimental ones. For both cases, VA and SA, the Freundlich model provided a better fitting to the experimental results.

The equilibrium adsorption capacity for each experiment of fixed bed (q_f) was calculated using the equation 16. An example of calculation for VA at 298 K with a C_f of 0.67 g/L and a t_{se} of 62.2 min (table 14) is presented below.

$$q_f = \frac{5.2 \times 0.67 \times 62.2}{4.4 \times (1-0.35) \times 1012 \times 0.32} - \frac{0.35 \times 0.67}{(1-0.35) \times 1012 \times 0.32} = 0.24 \text{ g/g } _{\text{dry resin}}$$

The column volume was 4.4 mL (volume of cylinder with a diameter 1 cm and the length 5.6 cm), the bed porosity was 0.35 and the humidity factor was of 0.68.

Thus, the adsorption capacity for VA with a concentration of 0.67 g/L at 298 K is 0.24 g/g.

The q_f values obtained to VA and SA in fixed bed adsorption are in table 16.

Table 16. *C_f and q_f values of VA and SA at 288, 298 and 313 K on fixed bed adsorption*

Compound	Temperature (K)	288	298	298	313
VA	C_f (mg/mL)	1.40	0.67	1.22	1.39
	q_f (g/g)	0.38	0.24	0.29	0.26
SA	C_f (mg/mL)	0.71	0.16	0.67	0.71
	q_f (g/g)	0.34	0.18	0.32	0.29

The isotherms with the batch and fixed bed results and fittings to Langmuir and Freundlich models for VA are presented in figure 20 and 21, respectively.

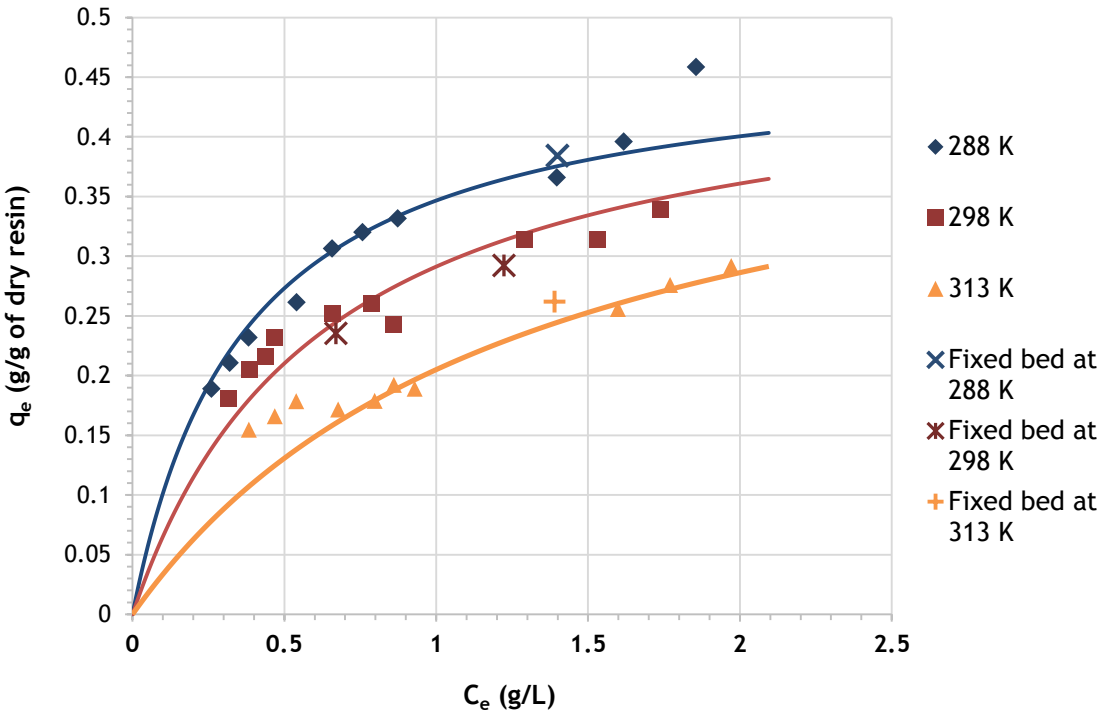

Figure 20. Experimental *adsorption equilibrium (symbols), q_e versus C_e, and fittings to the Langmuir model (lines) at different temperatures (288 K, 298 K and 313 K) for the adsorption of VA onto Sepabeads SP700. Fixed bed points resulting from feed concentration of 1.40 g/L (313 K), 1.22 g/L (298 K), 0.67 g/L (298 K) and 1.39 g/L (288 K) at flow-rate of 5.2 mL/min, are also shown*

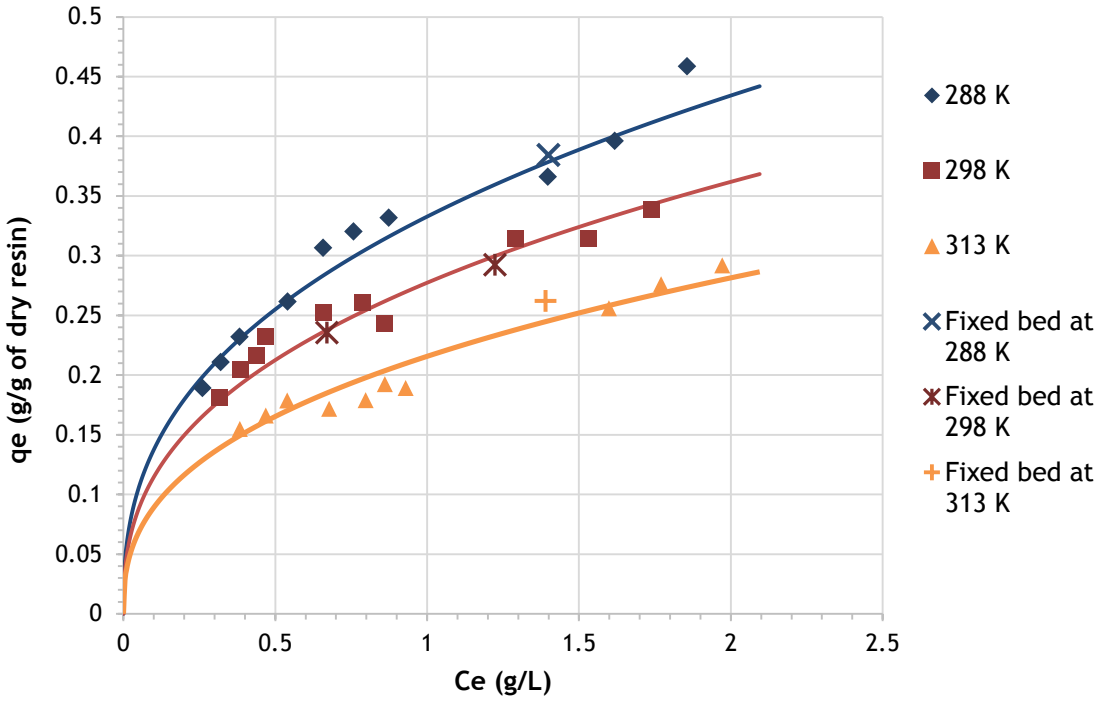

Figure 21. *Experimental adsorption equilibrium (symbols), q_e versus C_e, and fittings to the Freundlich model (lines) at different temperatures (288 K, 298 K and 313 K) for the adsorption of VA onto Sepabeads SP700. Fixed bed points resulting from feed concentration of 1.40 g/L (313 K), 1.22 g/L (298 K), 0.67 g/L (298 K) and 1.39 g/L (288 K) at flow-rate of 5.2 mL/min, are also shown*

It is visible by the adsorption equilibrium isotherms (figure 20 and 21) that the experimental results of fixed bed adsorption are better described by the Freundlich model. At 313 K, equilibrium capacity of adsorption obtained on fixed bed for VA present a deviation from the Freundlich model, leading to the experimental and theoretical stoichiometric time to be quite different for this temperature.

The experimental and theoretical q_f values and respective ERRQS of Langmuir and Freundlich model for VA are present in table 17.

Table 17. *Experimental and theoretical q_f values with ERRQS for Langmuir and Freundlich models for VA*

	Temperature (K)	288	298	298	313
	C_f (mg/mL)	1.40	0.67	1.22	1.39
Experimental	q_f (g/g)	0.38	0.24	0.29	0.26
Langmuir model	q_f (g/g)	0.38	0.24	0.31	0.24
	ERRQS	7.69×10^{-05}	9.07×10^{-05}	4.52×10^{-04}	3.24×10^{-04}
Freundlich model	q_f (g/g)	0.38	0.24	0.30	0.24
	ERRQS	3.15×10^{-05}	6.60×10^{-06}	5.74×10^{-05}	2.92×10^{-04}

Looking to the table 17, it is observed that the ERRQS values obtained for Freundlich model were lower than the values obtained for Langmuir model, proving once more that the adsorption behaviour at different temperatures is better described by Freundlich model.

The isotherms with the batch and fixed bed results and fitting to Langmuir and Freundlich model for SA are presented in figure 22 and 23, respectively.

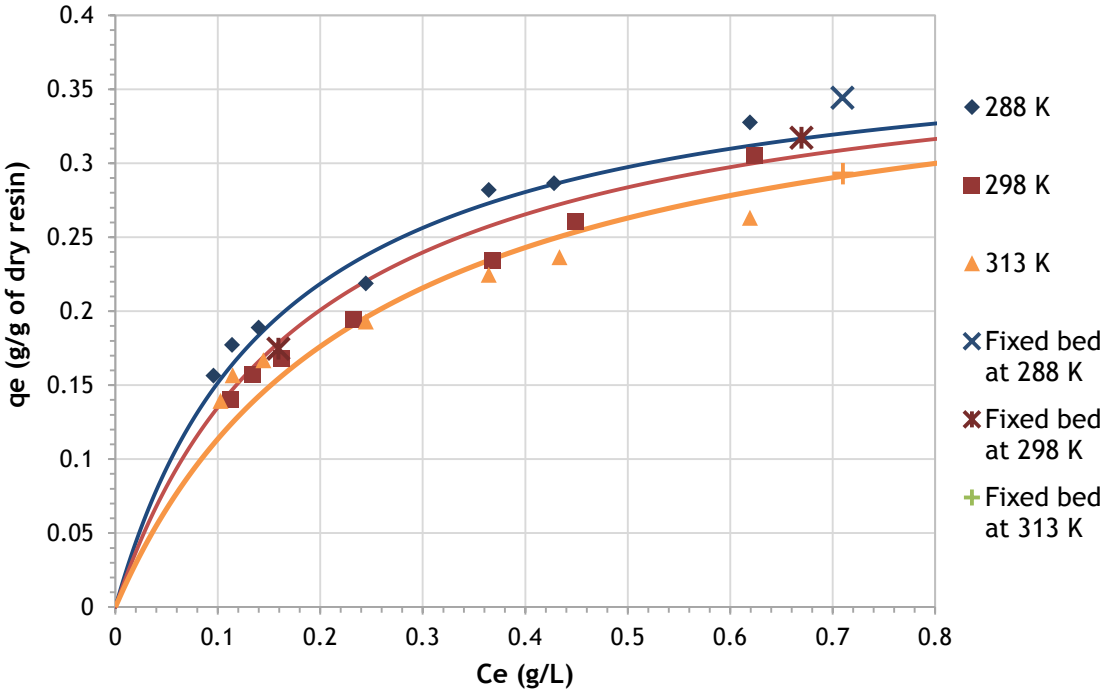

Figure 22. *Experimental adsorption equilibrium (symbols), q_e versus C_e, and fittings to the Langmuir model (lines) at different temperatures (288 K, 298 K and 313 K) for the adsorption of SA onto Sepabeads SP700. Fixed bed points resulting from feed concentration of 0.71 g/L (313 K), 0.67 g/L (298 K), 0.16 g/L (298 K) and 0.71 g/L (288 K) at flow-rate of 5.2 mL/min, are also shown*

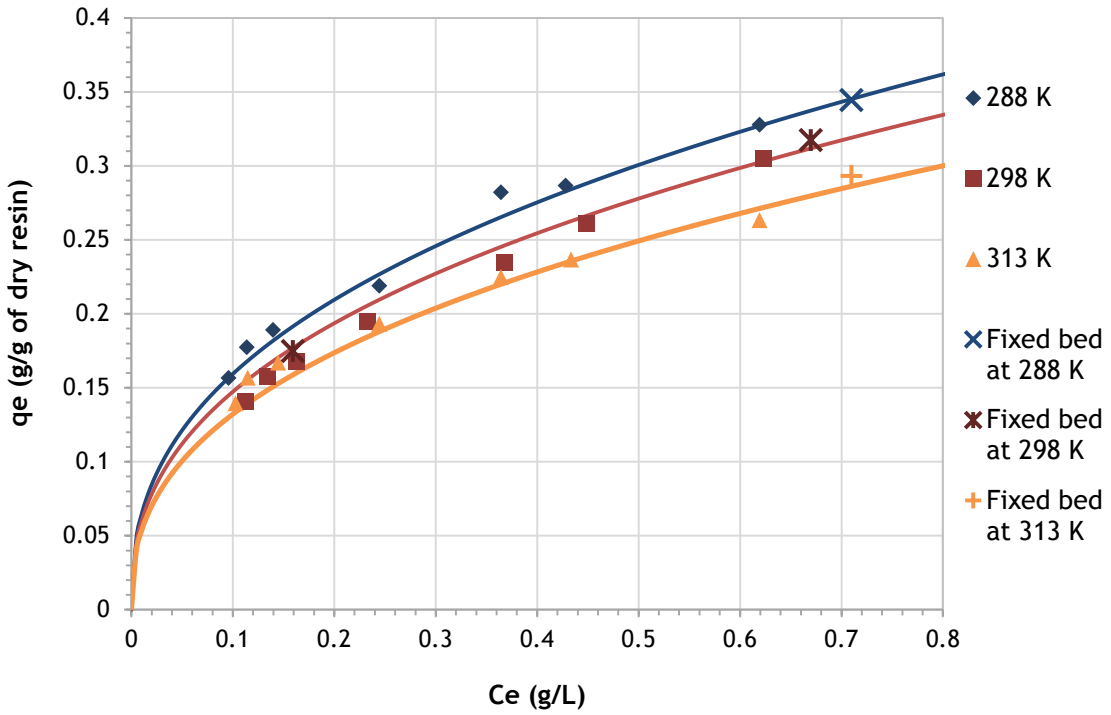

***Figure 23**. Experimental adsorption equilibrium (symbols), q_e versus C_e, and fittings to Freundlich model (lines) at different temperatures (288 K, 298 K and 313 K) for the adsorption of SA onto Sepabeads SP700. Fixed bed points resulting from feed concentration of 0.71 g/L (313 K), 0.67 g/L (298 K), 0.16 g/L (298 K) and 0.71 g/L (288 K) at flow-rate of 5.2 mL/min, are also shown*

The experimental and theoretical q_f values and respective ERRQS of Langmuir and Freundlich models for SA is present in table 18.

***Table 18**. Experimental and theoretical q_f values with ERRQS for Langmuir and Freundlich models for SA*

	Temperature (K)	288	298	298	313
	C_f (mg/mL)	0.71	0.16	0.67	0.71
Experimental	q_f (g/g)	0.34	0.18	0.32	0.29
Langmuir model	q_f (g/g)	0.32	0.18	0.30	0.29
	ERRQS	5.65×10^{-04}	1.26×10^{-05}	1.56×10^{-04}	1.03×10^{-05}
Freundlich model	q_f (g/g)	0.34	0.18	0.31	0.29
	ERRQS	1.09×10^{-06}	6.34×10^{-06}	2.76×10^{-05}	4.59×10^{-05}

Also in the case of SA, the Freundlich model presented a better fitting to the results of fixed bed and batch than Langmuir model.

For this model the equilibrium capacity of adsorption on fixed bed was very close to the values resulting from the Freundlich model.

5.3 Fixed-bed Desorption

After each stage of adsorption the resin was regenerated and the adsorbate was recovered. For this step it was used as eluent a solution of ethanol/water (90/10 v/v) and a flow rate of 5.2 mL/min during 30 minutes.

The behaviour of desorption for the temperatures studied (288, 298 and 313 K) for VA and SA is shown in figures 24 and 25, respectively.

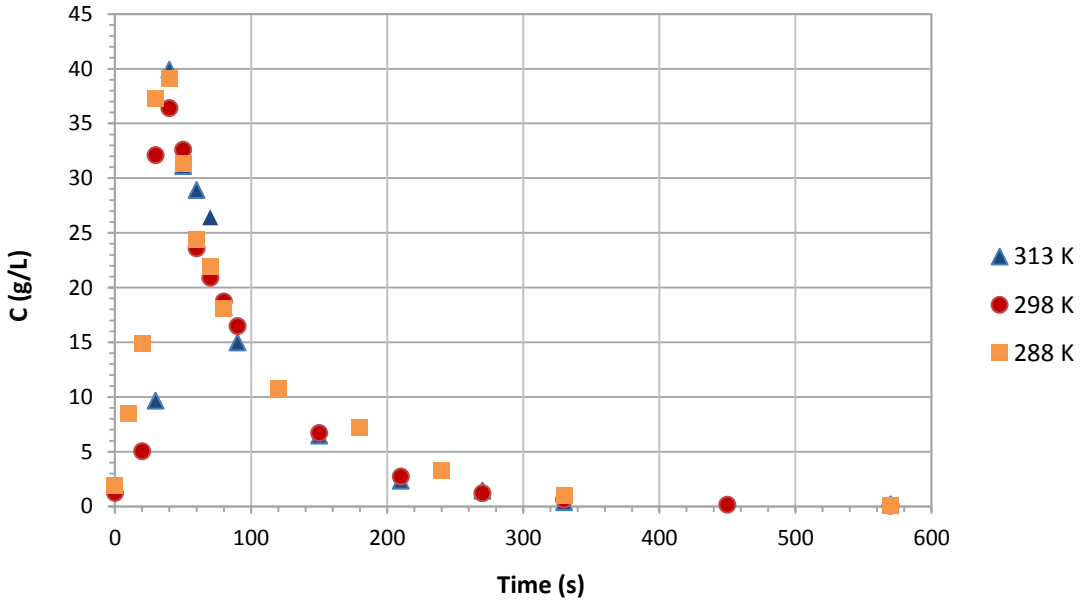

***Figure 24**. The outlet concentrations at different temperatures (288 K, 298 K and 313 K) of VA desorption onto Sepabeads SP700 at flow-rate of 5.2 mL/min*

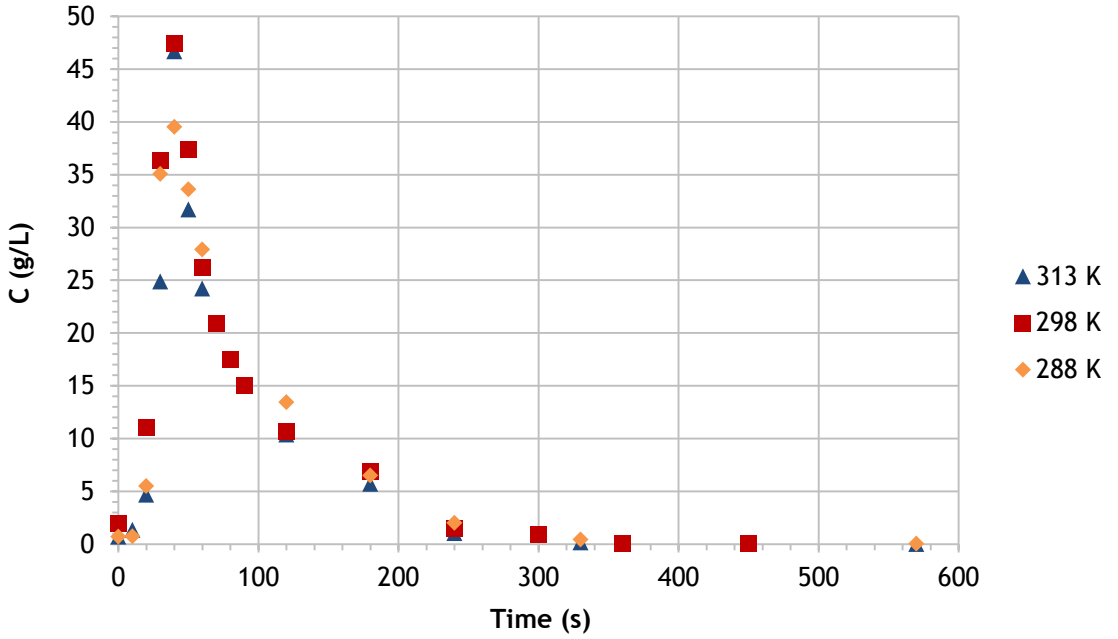

***Figure 25**. The outlet concentrations at different temperatures (288 K, 298 K and 313 K) of SA desorption onto Sepabeads SP700 at flow-rate of 5.2 mL/min*

The highest concentration of each compound at the outlet was found at 40 seconds. For 600 seconds of elution, the concentration at the outlet is near 0. This is a fast process, in particular when compared with adsorption.

The behaviour of desorption to the two concentrations studied at 298 K for VA and SA on adsorption is observed in figure 26 and 27, respectively.

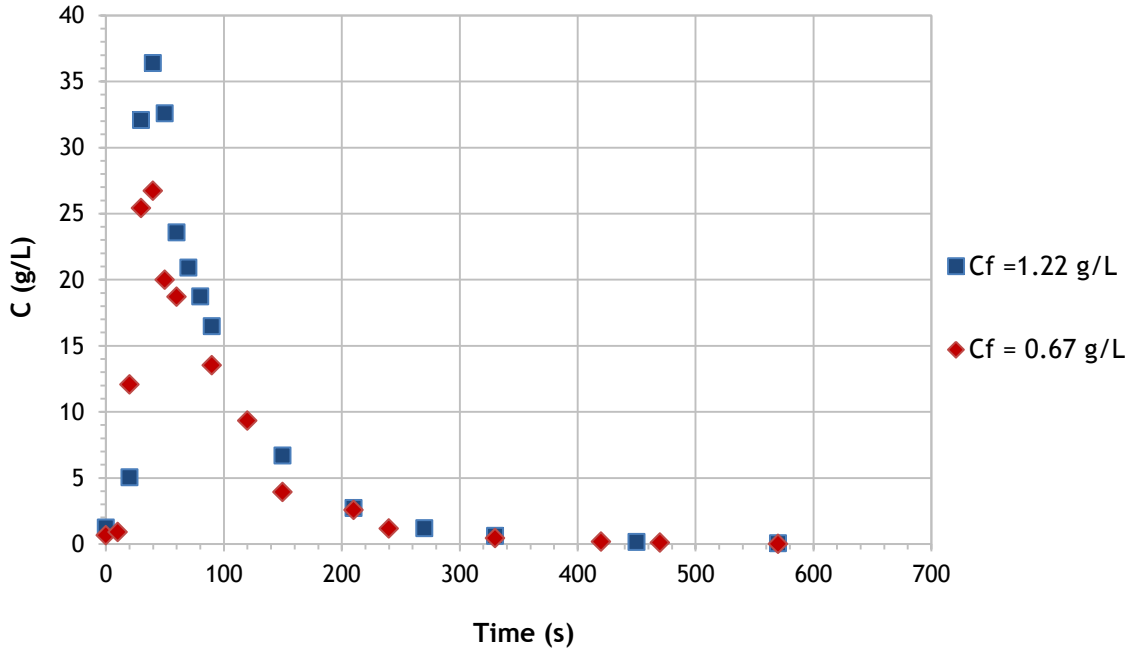

***Figure 26**. The outlet concentrations on desorption of VA onto Sepabeads SP700 at flow-rate of 5.2 mL/min for two feed concentrations of adsorption (1.22 g/L and 0.67 g/L)*

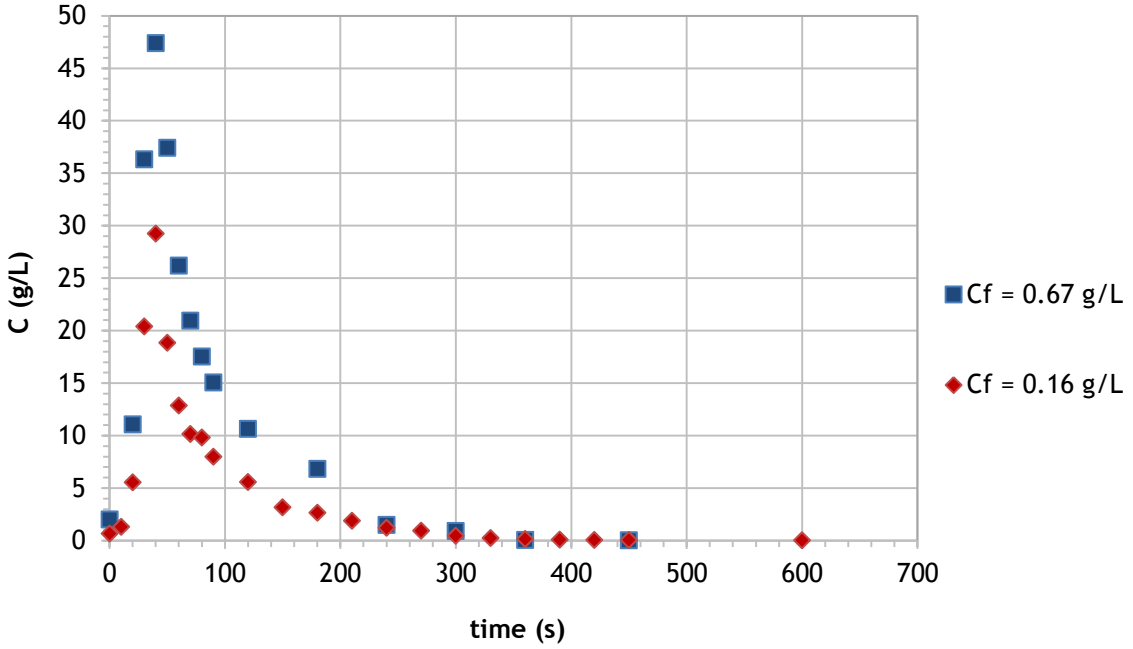

***Figure 27**. The outlet concentrations on desorption of **SA** onto Sepabeads SP700 at flow-rate of 5.2 mL/min for two feed concentrations of adsorption (0.67 g/L and 0.16 g/L).*

Figures 26 and 27 showed a similar behaviour of desorption for the two C_f values. The difference is the amount defined by the area bellow the desorption profile defined by the concentration, which is lower to the experiment with lower C_f.

The equilibrium desorption capacity for the VA and SA was calculated by the equation 17.
An example of calculation for VA with a C_f of 0.67 g/L is presented:

$$q_{des} = \frac{39 \times 5.2}{4.4 \times (1-0.35) \times 1012 \times 0.32} - \frac{0.35 \times 0.67}{(1-0.35) \times 1012 \times 0.32} = 0.22\ \text{g/g}$$

Thus, for the VA desorption with a concentration of 0.67 g/L, a flow rate of 5.2 mL/min and an area resulting from plot (C vs time) of 39 g min/L the desorption capacity was 0.22 g/g.

The areas obtained to each plot of C (g/L) versus time (min) in desorption is presented in appendix H (Table 33).

The results of desorption capacity for the two compounds are shown in table 19.

***Table 19**. Desorption capacity of VA and SA in fixed bed*

Compound	Temperature (K)	288	298	298	313
VA	C_f (mg/mL)	1.40	0.67	1.22	1.39
	q_{des} (g/g)	0.33	0.22	0.28	0.26
SA	C_f (mg/mL)	0.71	0.16	0.67	0.71
	q_{des} (g/g)	0.31	0.17	0.30	0.27

Comparing the table 19 with the table 16 it is observed that the values of adsorption and desorption capacity for the two compounds and for the temperatures studied are similar.

Next, it is presented the recovery percentage of VA and SA for 5 bed volumes, Table 20.

***Table 20**. Recovery percentage of VA and SA in the desorption*

Compound	*Temperature*	288	298	298	313
VA	C_f (g/L)	1.40	0.67	1.22	1.39
	Recovery (%)	85	93	94	95
SA	C_f (g/L)	0.71	0.16	0.67	0.71
	Recovery (%)	91	97	94	92

It is observed a recover superior at 90% for 5 bed volumes except for VA at 288 K. In a study reported in the literature for VL using a macroporous resin[26] it was achieved a recovery of more than 96% of the adsorbed VL using 5 bed volumes, which is within the range obtained in this work.

Comparing the adsorption capacity obtained for VA and SA with the adsorption capacity of SY and for VL studied by some authors,[22, 25, 27] it is possible to conclude that the acids have a similar behaviour of the aldehydes. However, a similar study that allows comparing directly the results of this work was not found.

6 Conclusions

Experiments of VA and SA adsorption onto Sepabeads SP700 (non-polar macroporous resin) were performed in batch and in fixed-bed. The effect of temperature on the adsorptive behaviour was evaluated. This study shows that Sepabeads SP700 resin can be employed as adsorbent to recover VA and SA from aqueous solution. The influence of temperature in adsorption of both compounds was also studied. The equilibrium adsorption capacity (q_e) of resin decreased with increasing of temperature. The q_e values were fitted to the Langmuir and Freundlich models. The maximum adsorption capacity obtained with the Langmuir model was 0.475 g/g to VA and 0.391 g/g to SA. With the Freundlich model, it was obtained a 1/n of 0.383 and 0.396 for VA and SA, respectively, indicating that the adsorption was favourable. Freundlich model predicted better the q_e values for VA and SA than Langmuir model.

The energies required to occur the sorption process were -34.2 and -13.1 kJ/mol for VA and SA, respectively. The negative values obtained allowed to conclude that the adsorption had an exothermic behaviour and it explained the reason for the increase of q_e values with the decrease of temperature. The phenolic acids had a similar behaviour of the aldehydes studied by some authors.

It was observed that the temperature had more effect on VA than on SA adsorption. The adsorption equilibrium isotherms at different temperatures were closer for SA indicating that the q_e was less affected by the temperature. However, the effect of temperature was more notorious for higher values of equilibrium concentrations.

The behaviour of the compounds in the fixed bed was similar to the static process and the q_e values could fit to the Freundlich model used in batch adsorption.

For a similar feed concentration (C_f) of VA (1.40 g/L) the q_f was 0.38 g/g for 288 K and 0.26 g/g for 313 K. For the same temperature (298 K), the q_f *was 0.24 for a* C_f of 0.67 g/L and 0.29 g/g for a C_f of 1.22 g/L.

To the SA, for the similar C_f *(0.71 g/L)* the q_f was 0.34 g/g for 288 K and 0.29 g/g for 313 K. For the same temperature (298 K), the q_f *was 0.18 for a* C_f of 0.16 g/L and 0.32 g/g for a C_f of 0.67 g/L.

In the end, studies of desorption were performed with ethanol/water (90/10, v/v). The maximum concentration in outlet was achieved at approximately 40 seconds and after that, it slowly decreased until zero. The values of adsorption and desorption capacity for the two compounds and for the temperatures studied are similar meaning that the compounds were readily desorbed with the ethanol solution. In the desorption process, it was possible to recover more than 90 % of adsorbed VA and SA using five bed volumes of ethanol/water (90/10, v/v), except for VA at 288 K that had a recover of 85 %.

7 Limitations and future work

The limitations that occurred during the experiments and suggestions about the work needed to complete this one presented.

VA and SA solutions were difficult to work due to crystallization (probably promoted by resin particles) even using concentrations in solution bellow the solubility limit. Due to this limitation, it was necessary to repeat experiments and, as such, it was required more time to carry out the experimental work.

The information about application of adsorption or other methods to recover these compounds from lignin is scarce. It is necessary to study the characteristics of the mixture, composition and possible interactions.

As proposal to future work, the study at higher range values of ratio between the adsorbate and the adsorbent should be done for the two compounds and applying the three temperatures to complete the adsorption isotherms and broaden the range of q_e and C_e.

The study of adsorption of VA and SA together and also with VL and SY, and real solution of lignin should be done to understand if it is possible to recover the four compounds directly by adsorption or if it is needed other process before adsorption.

Kinetic adsorption studies to the two compounds should be done.

8 References

[1] Report CELPA 2012 – Portuguese Paper Association, Available: http://www.tecnicelpa.com/. (accessed 20 june 2015)

[2] P.C.R. Pinto, A. E. Rodrigues, Oxidation of lignin from Eucalyptus globulus pulping liquors to produce syringaldehyde and vanillin, Industrial Engineering Chemistry Research, 52 (2013) 4421-4428.

[3] C.A.E. Costa, P.C.R. Pinto, A.E. Rodrigues, Evaluation of chemical processing impact on E. globulus wood lignin and comparison with bark lignin, Industrial Crops and Products, 61 (2014) 479-491.

[4] J.E. Holladay, J.J. Bozell, J.F. White, D. Johnson, Results of screening for potential candidates from biorefinery lignin, in Top Value-Added Chemicals from Biomass in, Pacific Northwest National Laboratory and National Renewable Energy Laboratory: Richland, WA., 2007.

[5] A.J. Ragauskas, G.T. Beckham, M.J. Biddy, R. Chandra, F. Chen, M.F. Davis, B.H. Davison, R.A. Dixon, P. Gilna, M. Keller, P. Langan, A.K. Naskar, J.N. Saddler, T.J. Tschaplinski, G.A. Tuskan, C.E. Wyman, Lignin Valorization: Improving lignin processing in the biorefinery, Science, 344 (2014).

[6] R.J.A. Gosselink, E. de Jong, B. Guran, A. Abächerli, Co-ordination network for lignin—standardisation, production and applications adapted to market requirements (EUROLIGNIN), Industrial Crops and Products, 20 (2004) 121-129.

[7] P.C.R. Pinto, E.A.B. Silva, A.E. Rodrigues, Lignin as source of fine chemicals: Vanillin and syringaldehyde, in: C. Baskar, S. Baskar, R.S. Dhillon (Eds.) Biomass Conversion, Springer Berlin Heidelberg, 2012, pp. 381-420.

[8] M. Norgren, H. Edlund, Lignin: Recent advances and emerging applications, Current Opinion in Colloid & Interface Science, 19 (2014) 409-416.

[9] M.L.A. Yrbas, F. Morucci, R. Alonso, S. Gorzalczany, Pharmalogical mechanism underlying the antinociceptive activity of vanillic acid, Pharmacology Biochemistry and Behaviour, 132 (2015) 88-95.

[10]K.R. Rekha, G.P.Selvakumar, K.I. Sivakamasundari, Effects of syringic acid on chronic MPTP/probenecid induced motor dysfunction, dopaminergic markers expression and neuroinflammation in C57BL/6 mice, Biomedicine & Aging Pathology, 4 (2014) 95-104.

[11] M.L. Soto, A. Moure, H. Domínguez, J.C. Parajó, Recovery, concentration and purification of phenolic compounds by adsorption: A review, Journal of Food Engineering, 105 (2011) 1-27.

[12] The Merck Index: An encyclopedia of chemicals, drugs and biologicals, New Jersey, 2001.

[13] C.L. Yaws, Thermophysical properties of chemicals and hydrocarbons, William Andrew Publishing, New York, United States of America, 2009.

[14] W.M. Haynes, D.R. Lide, The CRC Handbook of Chemistry and Physics, 85th ed, CRC, Florida, United States of America, 2004.

[15] Hangzhou weiku information & Technology Co. Ltd, Look for Chemicals, 2008, Available: http://weiku.company.weiku.com/. (accessed 20 june 2015)

[16] Chemical Book, 2008, Available: http://www.chemicalbook.com/. (accessed 20 june 2015)

[17] M. Ragnar, C.T. Lindgren, N.-O. Nilvebrant, pKa-values of guaiacyl and syringyl phenols related to lignin, Journal of Wood Chemistry and Technology, 20 (2000) 277-305.

[18] A. Noubigh, A. Mgaidi, M. Abderrabba, E. Provost, W. Fürst, Effect of salts on the solubility of phenolic compounds: experimental measurements and modelling, Journal of the Science of Food and Agriculture, 87 (2007) 783-788.

[19] Royal Society of Chemistry, ChemSpider - search and share chemistry, 2014, Available: http://www.chemspider.com/. (accessed 22 june 2015)

[20] M. Ahmaruzzaman, Adsorption of phenolic compounds on low-cost adsorbents: A review, Advances in Colloid and Interface Science, 143 (2008) 48-67; G. Dong, J. Xu, Y. Gu, Y. Wei, A general separation method of phenolic acids using pH-zone-refining counter-current chromatography and its application to oat bran, Journal of Chromatography B, 992 (2015) 36-42.

[21] J.F. García-Araya, F.J. Beltrán, P. Álvarez, F.J. Masa, Activated carbon adsorption of some phenolic compounds present in agroindustrial wastewater, Adsorption, 9 (2003) 107-115.

[22] C. Michailof, G.G. Stavropoulos, C. Panayiotou, Enhanced adsorption of phenolic compounds, commonly encountered in olive mill wastewaters, on olive husk derived activated carbons, Bioresource Technology, 99 (2008) 6400-6408.

[23] D. Richard, M.L. Delgado-Núñez, D. Schweich, Adsorption of complex phenolic compounds on active charcoal: Adsorption capacity and isotherms, Chemical Engineering Journal, 148 (2009) 1-7.

[24] V.P. Ravi, R.V. Jasra, T.S.G. Bhat, Adsorption of phenol, cresol isomers and benzyl alcohol from aqueous solution on activated carbon at 278, 298 and 323 K, Journal of Chemical Technology and Biotechnology, 71 (1998) 173-179.

[25] Z. Wang, K. Chen, J. Li, Q. Wang, J. Guo, Separation of vanillin and syringaldehyde from oxygen delignification spent liquor by macroporous resin adsorption, Clean - Soil, Air, Water, 38 (2010) 1074-1079.

[26] Q.F. Zhang, Z.T. Jiang, H.J. Gao, R. Li, Recovery of vanillin from aqueous solutions using macroporous adsorption resins, European Food Research and Technology, 226 (2008) 377-383.

[27] M. Zabkova, M. Otero, M. Minceva, M. Zabka, A.E. Rodrigues, Separation of synthetic vanillin at different pH onto polymeric adsorbent Sepabeads SP206, Chemical Engineering and Processing: Process Intensification, 45 (2006) 598-607.

[28] E. Conde, A. Moure, H. Domínguez, M.H. Gordon, J.C. Paraj, Purified phenolics from hydrothermal treatments of biomass: ability to protect sunflower bulk oil and model food emulsions from oxidation, Journal of Agricultural and Food Chemistry, 59 (2011) 9158–9165.

[29] B. Díaz-Reinoso, N. González-López, A. Moure, H. Domínguez, J.C. Parajó, Recovery of antioxidants from industrial waste liquors using membranes and polymeric resins, Journal of Food Engineering, 96 (2010) 127-133.

[30] M.L. Soto, E. Conde, N. González-López, M.J. Conde, A. Moure, J. Sineiro, E. Falqué, H. Domínguez, M. J. Núñez, J.C. Parajó, Recovery and concentration of antioxidants from winery wastes molecules, 17 (2012) 3008-3024.

[31] J.F. Richardson, J.H. Harker, J.R. Backhurst, Coulson and Richardson's Chemical Engineering Volume 2 - Particle technology and separation processes (5th Edition), in, Elsevier, 2002.

[32] D.O. Cooney, Adsorption design for wastewater treatment, Lewis Publishers, Florida, United States of America, 1999.

[33] E. Worch, Adsorption technology in water treatment: Fundamentals, processes, and modeling, walter de gruyter, Dresden, Germany, 2012.

[34] X. Geng, P. Ren, G. Pi, R. Shi, Z. Yuan, C. Wang, High selective purification of flavonoids from natural plants based on polymeric adsorbent with hydrogen-bonding interaction, Journal of Chromatography A, 1216 (2009) 8331-8338.

[35] K.Y. Foo, B.H. Hameed, Insights into the modeling of adsorption isotherm systems, Chemical Engineering Journal, 156 (2010) 2-10.

[36] F. Gimbert, N. Morin-Crini, F. Renault, P.-M. Badot, G. Crini, Adsorption isotherm models for dye removal by cationized starch-based material in a single component system: Error analysis, Journal of Hazardous Materials, 157 (2008) 34-46.

[37] G. Guiochon, A. Felinger, D.G.G. Shirazi, A.M. Katti, Fundamentals of preparative and nonlinear chromatography, 2nd ed., Elsevier, 2006.

[38] I. Langmuir, The adsorption of gases on plane surfaces of glass, mica and platinum, Journal of American Chemical Society, 40 (1918) 1361-1402.

[39] Freundlich, H. M. F. Kapillarchemieeds. Akademische Verlagsgesellschaft: Leipzig,Germany, 1909.

[40] K.V. Kumar, K. Porkodi, F. Rocha, Comparison of various error functions in predicting the optimum isotherm by linear and non-linear regression analysis for the sorption of basic red 9 by activated carbon, Journal of Hazardous Materials, 150 (2008) 158-165; Y.-S. Ho, Selection of optimum sorption isotherm, Letters to the Editor / Carbon, 42 (2004) 2113–2130.

[41] D.M. Ruthven, Principles of adsorption and adsorption processes, John Willey and Sons, New York, United States of America, 1984.

[42 A. Ozcan, A.S. Ozgan, O. Gok, Adsorption kinetics and isotherms of anionic dye of reactive blue 19 from aqueous solutions onto DTMA-Sepiolite, in: A.A. Lewinsky (Ed.) Hazardous Materials and Wastewater: Treatment, Removal and Analysis , Nova Science Publisher, Inc., New York, United States of America, 2006, pp. 225-249

[43] A. D. Site, Factors affecting sorption of organic compounds in natural sorbent/water systems and sorption coefficients for selected pollutants. A Review, Journal of Physical and Chemical Reference Data, 30 (2001) 187-439.

[44] J. Kammerer, R. Carle, D.R. Kammerer, Adsorption and ion exchange: basic principles and their application in food processing, Journal of Agricultural and Food Chemistry, 59 (2010) 22-42.

[45] Adsorption: Science and Technology, Proceedings of the NATO advanced study institute on adsorption: science and technology , A. E. Rodrigues, M.D.LeVan,.D.Tondeur. (Ed.) NATO ASI Series, Series E: Applied Sciences, Vol. 158, Kluwer Academic Publisher, 1989.

[46] A.E.R. Mónica, P.S. Santos, Adsorption equilibrium and fixed bed adsorption of aniline onto polymeric resin and activated carbons, Separation Science and Technology, (2014).

[47] D.R. Nielsen, G.S. Amarasiriwardena, K.L. Prather Predicting the adsorption of second generation biofuels by polymeric resins with applications for in situ product recovery (ISPR). Bioresource Technology, 101 (2010) 2762-2769.

9 Appendix

9.1 Appendix A

Figure 28 presents the calibrations curves obtained to VA and SA.

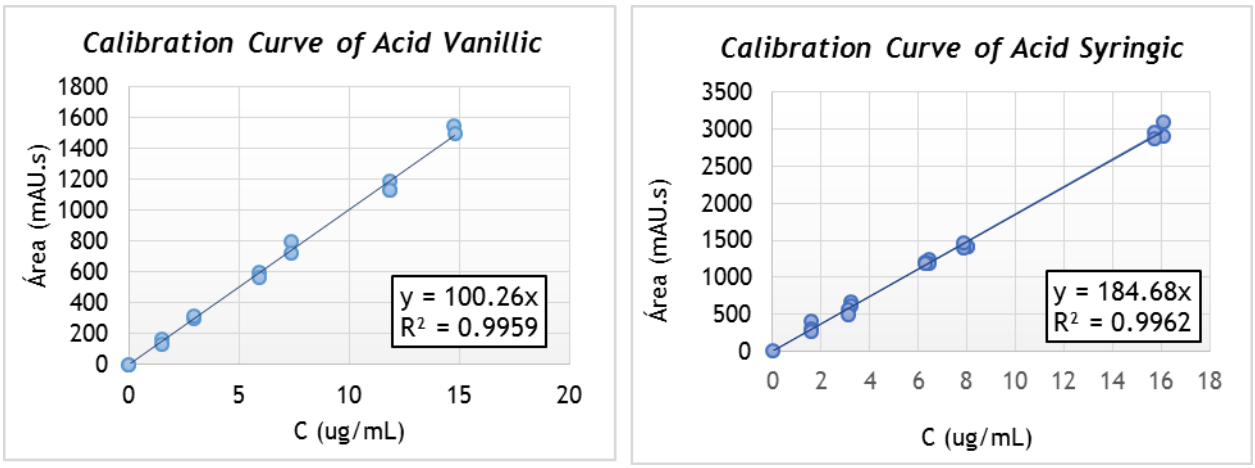

***Figure 28**. Calibration curve of VA and SA*

9.2 Appendix B

The solubility obtained for VA is presented in table 21.

***Table 21**. Solubility for different temperatures for VA*

Temperature (K)	Number of filters	Concentration medium in solution (mg/mL)
295 (room temperature)	2	3.06
298	3	3.21
288	4	3.07

The solubility obtained for SA is presented in table 22.

***Table 22**. Solubility for different temperatures for SA*

Temperature (K)	Number of filters	Concentration medium in solution (mg/mL)
295 (room temperature)	2	3.13
298	3	2.02
288	4	1.17

The solubility in water of SA and VA were tested. Table 23 shows that the temperature did not affect the concentration of VA in solution, but it was always visible turvation in solution before the filtrations, decreasing with temperature rise. The filtrations made did not affect the concentration of VA, thus the turbidity probably was caused by impurities.

Observing the table 22, it is visible that the concentration of SA in solution decrease with the decrease of temperature, thus the solubility of SA is affected by the temperature on the opposite to VA.

9.3 Appendix C

In this appendix is present the C_o *of* VA, resin weight and the ratios for each experiment.

***Table 23**. Ratio of VA weight and resin weight for isotherm determination at 288 K*

Experiment	VA C_0 (mg/L)	Resin mass (mg)	mg compound/mg resin
1.1	1149	267	0.430
1.2	1149	517	0.222
1.3	1149	750	0.153
1.4	1020	264	0.386
1.5	1020	887	0.115
1.6	1020	1071	0.095
1.7	1020	1296	0.079
2.1	2248	276	0.815
2.2	2248	514	0.437
2.3	2248	750	0.300

In the next table, it is presented the ratio of VA weight and resin weight for the experiments at 298 K.

***Table 24**. Ratio of VA weight and resin weight for isotherm determination at 298 K*

Experiment	VA C_0 (mg/L)	Resin mass (mg)	mg compound/mg resin
1.1	1050	253	0.415
1.2	1050	502	0.209
1.3	1050	765	0.137
1.4	1020	289	0.353
1.5	1020	868	0.118
1.6	1020	1001	0.102
1.7	1020	1251	0.082
2.1	2015	261	0.772
2.2	2015	510	0.395
2.3	2015	751	0.268

Next, it is presented the ratio of VA and resin weights for the experiment at 313 K.

***Table 25**. Ratio of VA weight and resin weight for isotherm determination at 313 K*

Experiment	VA C_0 (mg/L)	Resin mass (mg)	mg compound/mg resin
1.1	1083	258	0.420
1.2	1083	513	0.211
1.3	1083	761	0.142
1.4	1020	266	0.383
1.5	1020	867	0.118
1.6	1020	1071	0.095
1.7	1020	1326	0.077
2.1	2208	260	0.848
2.2	2208	512	0.432
2.3	2208	767	0.288

9.4 Appendix D

In this appendix is present the C_0 of SA, the resin weight and the ratio for each experiment.

***Table 26**. Ratio of SA weight and resin weight for isotherm determination at 288 K.*

Experiment	SA C_0 (mg/L)	Resin mass (mg)	mg compound/mg resin
1.1	585	252	0.232
1.2	585	501	0.117
1.3	585	759	0.077
1.4	585	856	0.068
1.5	585	1007	0.058
2.1	877	254	0.346
2.2	877	506	0.173

In the next table, it is presented the ratio of SA weight and resin weight for the experiments at 298 K.

***Table 27**. Ratio of SA weight and resin weight for isotherm determination at 298 K.*

Experiment	SA C_0 (mg/L)	Resin mass (mg)	mg compound/mg resin
1.1	554	257	0.216
1.2	554	535	0.104
1.3	554	754	0.074
1.4	554	862	0.064
1.5	554	1016	0.055
2.1	871	259	0.336
2.2	871	522	0.167

Next, it is presented the ratio of SA and resin weights for the experiment at 313 K.

***Table 28**. Ratio of SA weight and resin weight for isotherm determination at 313 K.*

Experiment	SA C_0 (mg/L)	Resin mass (mg)	mg compound/mg resin
1.1	542	265	0.204
1.2	542	509	0.107
1.3	542	769	0.071
1.4	542	880	0.062
1.5	542	1017	0.053
2.1	825	252	0.327
2.2	825	534	0.155

9.5 Appendix E

The table 29 shows the ERRSQ values obtained by fitting the q_e values by the Langmuir model to VA.

***Table 29**. ERRSQ values of fitting q_e to Langmuir model for VA*

	Temperature (K)		
Experiment	288	298	313
1.1	4.41×10^{-06}	9.91×10^{-04}	5.81×10^{-05}
1.2	4.82×10^{-06}	8.96×10^{-05}	1.94×10^{-07}
1.3	4.42×10^{-04}	8.69×10^{-04}	9.68×10^{-05}
1.4	7.56×10^{-07}	1.29×10^{-05}	1.72×10^{-05}
1.5	9.64×10^{-05}	4.30×10^{-04}	1.62×10^{-03}
1.6	1.07×10^{-04}	5.95×10^{-04}	1.68×10^{-03}
1.7	6.08×10^{-05}	4.53×10^{-04}	2.24×10^{-03}
2.1	3.92×10^{-03}	2.29×10^{-07}	4.83×10^{-05}
2.2	9.22×10^{-05}	5.00×10^{-04}	1.23×10^{-05}
2.3	8.67×10^{-05}	2.46×10^{-05}	2.09×10^{-05}
Sum	$\mathbf{4.82\times10^{-03}}$	$\mathbf{3.96\times10^{-03}}$	$\mathbf{5.80\times10^{-03}}$

*see tables 25, 26, 27 for initial conditions

The table 30 shows the ERRSQ values obtained by fitting the q_e values by the Freundlich model to VA.

***Table 30**. ERRSQ values of fitting qe to Freundlich model for VA*

	Temperature (K)		
Experiment	288	298	313
1.1	2.43×10^{-04}	3.67×10^{-04}	4.32×10^{-04}
1.2	5.26×10^{-04}	2.53×10^{-04}	3.60×10^{-04}
1.3	2.70×10^{-06}	6.13×10^{-04}	2.10×10^{-04}
1.4	4.37×10^{-04}	5.15×10^{-05}	1.36×10^{-04}
1.5	3.11×10^{-06}	1.86×10^{-04}	6.78×10^{-05}
1.6	2.07×10^{-05}	1.53×10^{-04}	1.99×10^{-05}
1.7	9.48×10^{-05}	4.40×10^{-06}	2.77×10^{-05}
2.1	1.33×10^{-03}	1.81×10^{-05}	1.36×10^{-04}
2.2	1.87×10^{-05}	1.62×10^{-04}	5.17×10^{-05}
2.3	1.52×10^{-04}	6.65×10^{-05}	6.11×10^{-06}
Sum	$\mathbf{2.83\times10^{-03}}$	$\mathbf{1.88\times10^{-03}}$	$\mathbf{1.45\times10^{-03}}$

*see tables 25, 26, 27 for initial conditions

The table 31 shows the ERRSQ values obtained by fitting the q_e values by the Langmuir model to SA.

***Table 31**. ERRSQ values of fitting qe to Langmuir model for SA*

	Temperature (K)		
Experiment	288	298	313
1.1	8.06×10^{-05}	5.72×10^{-04}	9.49×10^{-05}
1.2	3.57×10^{-04}	4.57×10^{-04}	7.77×10^{-06}
1.3	2.63×10^{-05}	1.64×10^{-04}	4.44×10^{-04}
1.4	1.78×10^{-04}	2.20×10^{-05}	9.97×10^{-04}
1.5	7.25×10^{-05}	3.46×10^{-05}	5.42×10^{-04}
2.1	2.44×10^{-04}	2.40×10^{-05}	3.15×10^{-04}
2.2	2.65×10^{-07}	2.09×10^{-04}	1.95×10^{-04}
Sum	$\mathbf{9.58\times10^{-04}}$	$\mathbf{1.48\times10^{-03}}$	$\mathbf{2.59\times10^{-03}}$

*see tables 28, 29, 30 for initial conditions

The table 32 shows the ERRSQ values obtained by fitting the q_e values by the Freundlich model to SA.

***Table 32**. ERRSQ values of fitting q_e to Freundlich model for SA*

	Temperature (K)		
Experiment	288	298	313
1.1	2.85×10^{-04}	1.56×10^{-04}	8.87×10^{-06}
1.2	5.96×10^{-05}	1.41×10^{-04}	1.31×10^{-05}
1.3	4.97×10^{-05}	1.25×10^{-04}	1.60×10^{-04}
1.4	9.13×10^{-05}	7.25×10^{-05}	2.58×10^{-04}
1.5	1.18×10^{-07}	2.21×10^{-04}	2.09×10^{-05}
2.1	6.45×10^{-07}	1.46×10^{-06}	1.03×10^{-04}
2.2	1.56×10^{-05}	3.93×10^{-05}	8.06×10^{-07}
Sum	$\mathbf{5.02\times10^{-04}}$	$\mathbf{7.56\times10^{-04}}$	$\mathbf{5.64\times10^{-04}}$

*see tables 28, 29, 30 for initial conditions

9.6 Appendix F

The figures 29, 30 and 31 represent the evolution of concentration o A in solution with time at 288, 298 and 313 K, respectively, for the experiments indicated in appendix C.

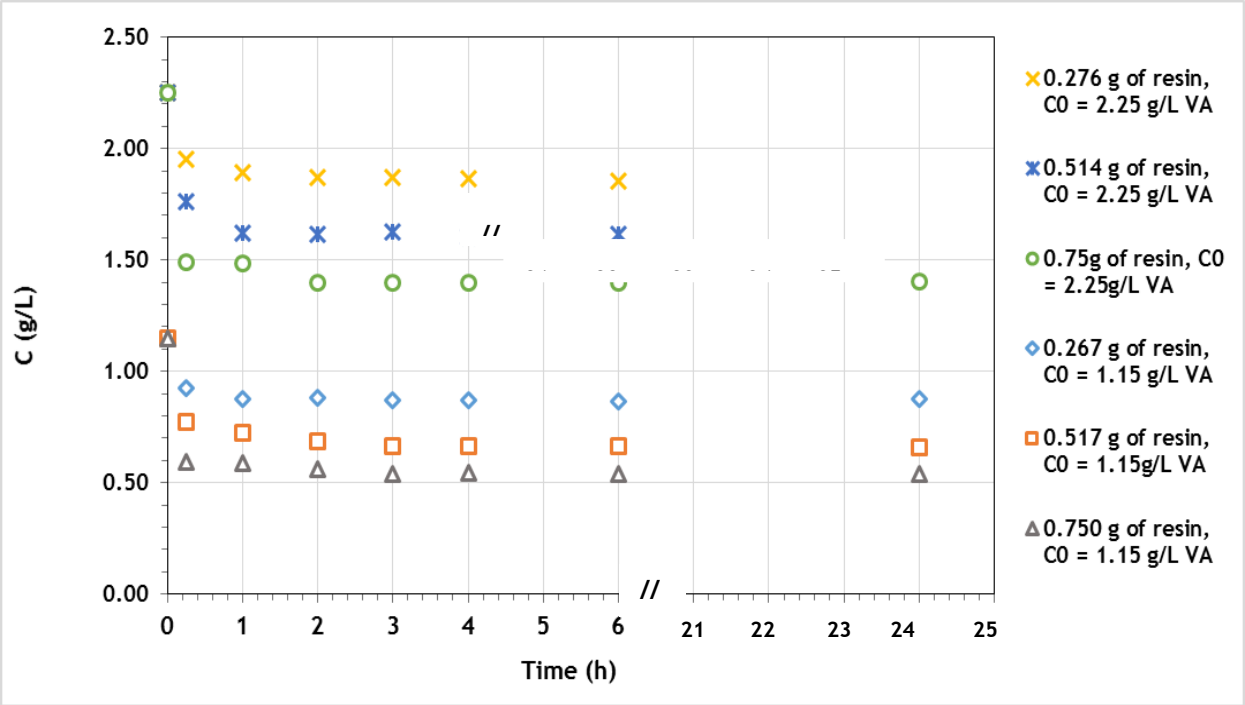

***Figure 29**. Variation of VA concentration with the time during the batch adsorption at 288 K*

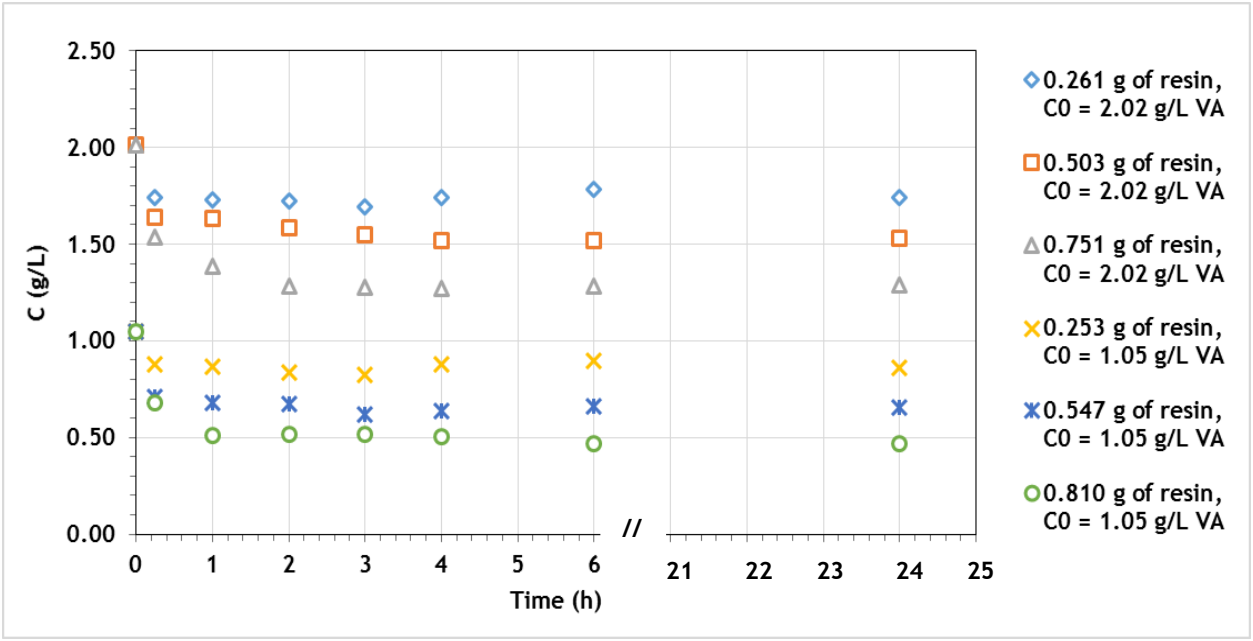

***Figure 30**. Variation of VA concentration with the time during the batch adsorption at 298 K*

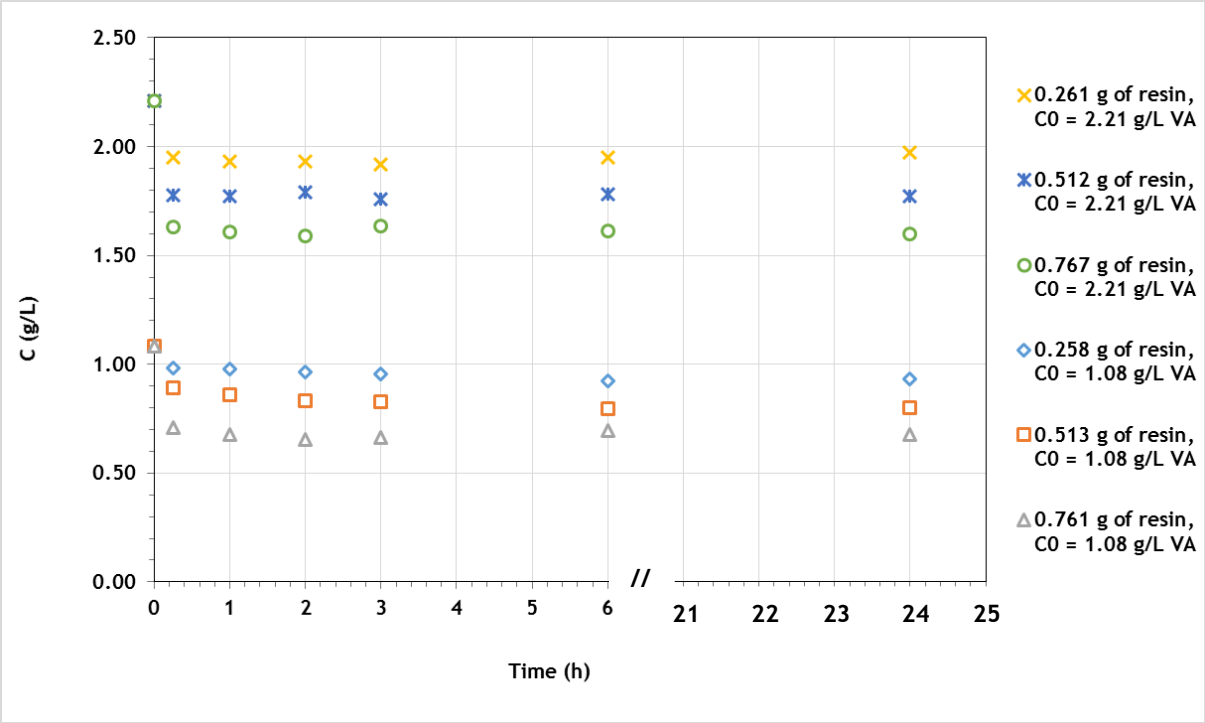

***Figure 31**. Variation of VA concentration with the time during the batch adsorption at 313 K*

9.7 Appendix G

The figures 32, 33 and 34 represent the evolution of concentration of SA in solution with time at 288, 298 and 313 K., respectively.

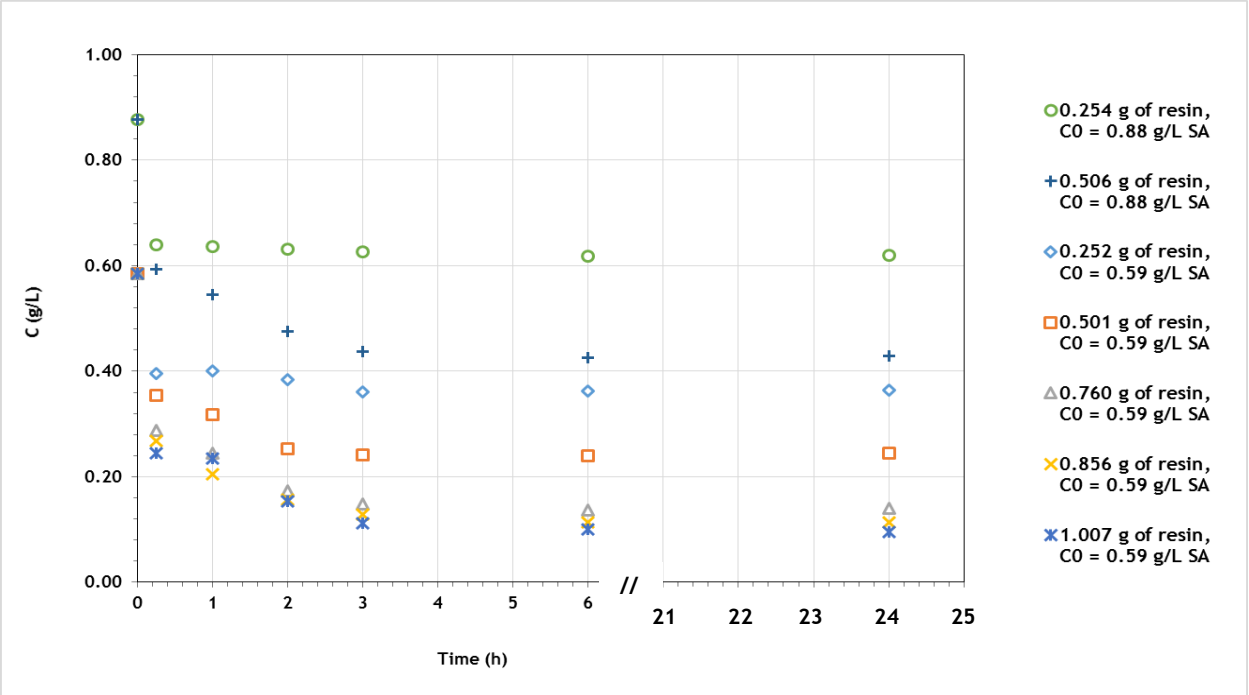

***Figure 32**.Variation of SA concentration with the time during the batch adsorption at 288 K*

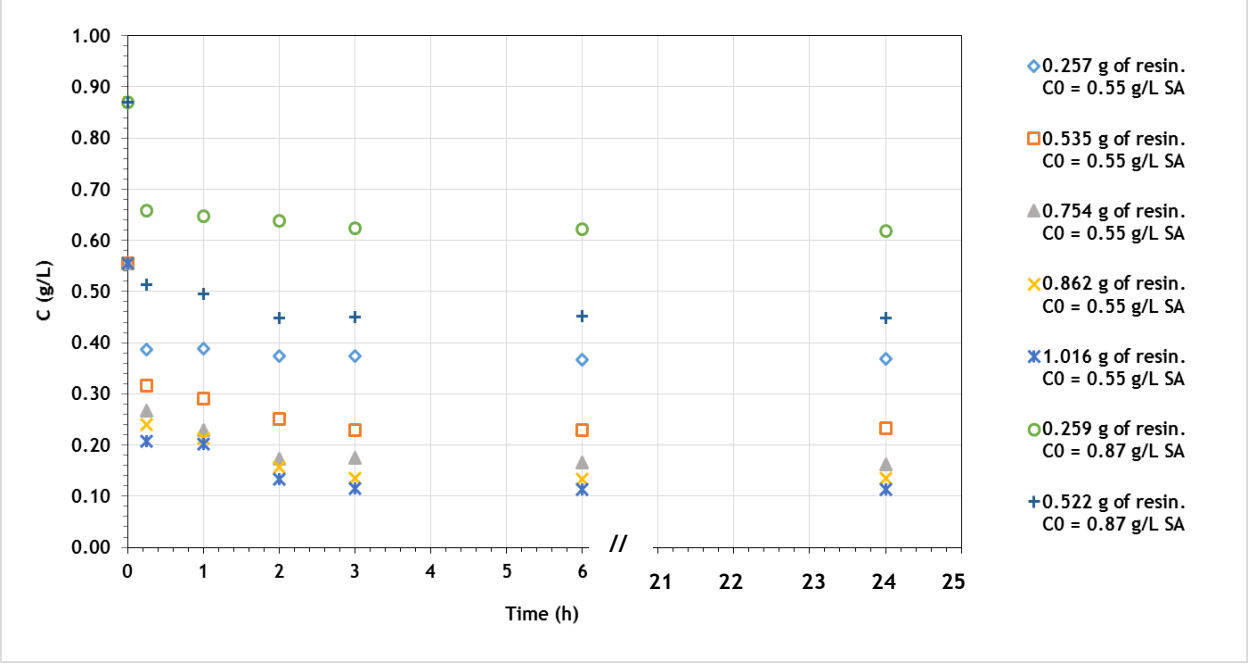

***Figure 33**. Variation of SA concentration with the time during the batch adsorption at 298 K*

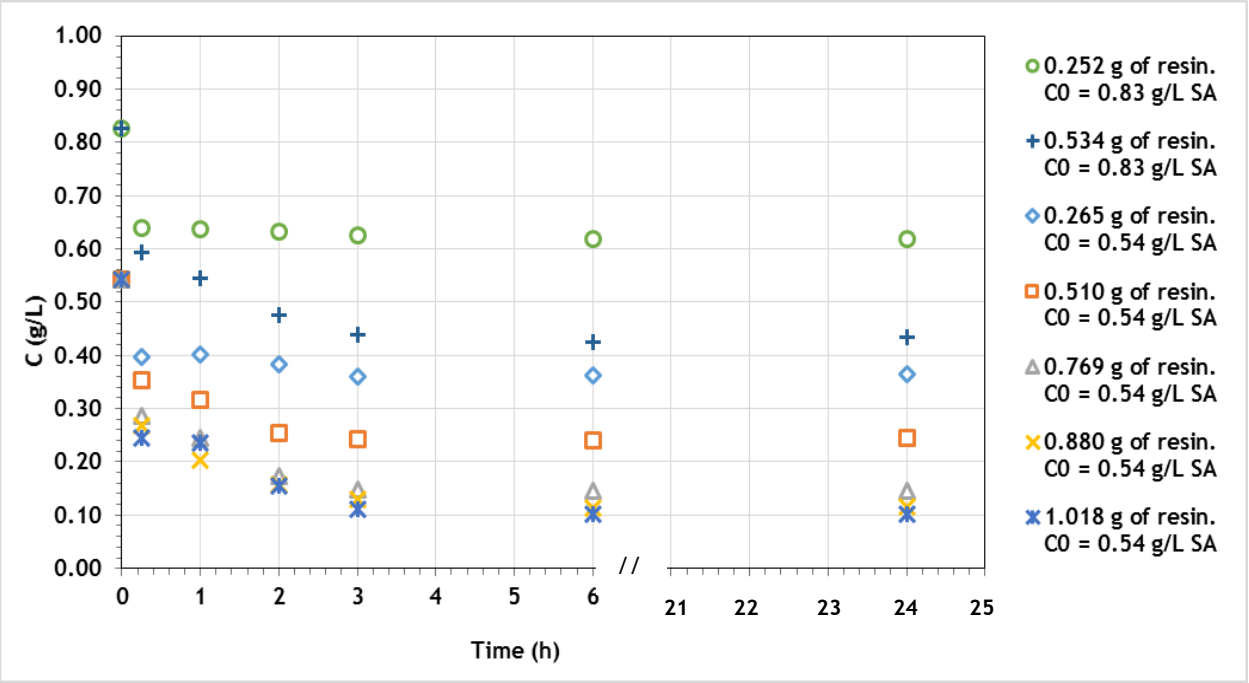

Figure 34. *Variation of SA concentration with the time during the batch adsorption at 313 K*

9.8 Appendix H

The areas obtained by plot of concentration versus time in desorption is presented in Table 33.

***Table 33**. Areas obtained in plot C vs time for VA and SA in desorption*

Compound	Temperature (K)	288	298	298	313
VA	C_f (mg/mL)	1.40	0.67	1.22	1.39
	Area (g.min/L)	58.3	37.1	49.4	46.4
SA	C_f (mg/mL)	0.71	0.16	0.67	0.71
	Area (g.min/L)	58.2	29.9	55.8	50.2